

# Semi-inclusive deep inelastic lepton scattering off complex nuclei

C. Ciofi degli Atti<sup>1</sup>, L.P. Kaptari<sup>1,a</sup>, S. Scopetta<sup>2</sup><sup>1</sup> Department of Physics, University of Perugia and Istituto Nazionale di Fisica Nucleare, Sezione di Perugia, Via A. Pascoli, I-06100 Perugia, Italy<sup>2</sup> Departament de Física Teòrica, Universitat de València, E-46100 Burjassot, València, Spain

Received: 4 March 1999

Communicated by B. Povh

**Abstract.** It is shown that in semi-inclusive deep inelastic scattering (DIS) of electrons off complex nuclei, the detection, in coincidence with the scattered electron, of a nucleus ( $A - 1$ ) in the ground state, as well as of a nucleon and a nucleus ( $A - 2$ ), also in the ground state, may provide unique information on several long standing problems, such as: *i*) the nature and the relevance of the final state interaction in DIS; *ii*) the validity of the spectator mechanism in DIS; *iii*) the medium induced modifications of the nucleon structure function; *iv*) the origin of the *EMC* effect.

**PACS.** 13.40.-f Electromagnetic processes and properties – 21.60.-n Nuclear-structure models and methods – 24.85.+p Quarks, gluons, and QCD in nuclei and nuclear processes – 25.60.Gc Breakup and momentum distributions

## 1 Introduction

In spite of many experimental and theoretical efforts (for a recent review see [1]), the origin of the nuclear EMC effect has not yet been fully clarified, and the problem as to whether the quark distributions of nucleons undergo deformations due to the nuclear medium remains open. Understanding the origin of the EMC effect would be of great relevance in many respects; consider, for example, that most QCD sum rules and predictions require the knowledge of the neutron quark distributions, which can only be extracted from nuclear experiments; this implies, from one side, a reliable knowledge of various nuclear quantities, such as the nucleon removal energy and momentum distributions, and, from the other side, a proper treatment of the lepton-nucleus reaction mechanism, including the effect of final state interaction (FSI) of the leptoproduced hadrons with the nuclear medium. Since the  $Q^2$  and  $x$ -dependences of the EMC effect is smooth, the measurements of the nuclear quark distributions in inclusive deep inelastic scattering (DIS) processes have not yet established enough constraints to distinguish between different theoretical approaches. In order to progress in this field, one should go beyond inclusive experiments, e.g. by considering semi-inclusive experiments in which another particle is detected in coincidence with the scattered electron. Most of the theoretical studies in this field concentrated on the process  $D(e, e'N)X$ , where  $D$  denotes the deuteron,  $N$  a nucleon, and  $X$  the undetected hadronic state. Current

theoretical models of this process are based upon the impulse approximation (IA) (also called *the spectator model*), according to which  $X$  results from DIS on one of the two nucleons in the deuteron, with  $N$  recoiling without interacting with  $X$  and being detected in coincidence with the scattered electron (for an exhaustive review see [2]). The model has been improved by introducing FSI [3], as well as by considering deviations from the spectator model by assuming that the detected nucleon originates from quark hadronisation [4, 5]. The semi-inclusive process on the deuteron  $D(e, e'N)X$ , on which experimental data will soon be available [6], could not only clarify the origin of the EMC effect, but, as illustrated in [7], could also provide more reliable information on the neutron structure function.

The spectator model has also been extended to complex nuclei by considering the process  $A(e, e'N)X$ , and by assuming that DIS occurs on a nucleon of a correlated pair, with the second nucleon  $N$  recoiling and being detected in coincidence with the scattered electron [5]. In the present paper two new types of semi-inclusive processes on complex nuclei will be considered, namely: i) the process  $A(e, e'(A - 1))X$ , in which DIS occurs on a mean-field, low-momentum nucleon, and the nucleus ( $A - 1$ ) recoils with low momentum and low excitation energy and is detected in coincidence with the scattered electron (note that for  $A = 2$  such a process coincides with the process  $D(e, e'N)X$  discussed previously); ii) the process  $A(e, e'N_2(A - 2))X$ , in which DIS occurs on a high momentum nucleon  $N_1$  of a correlated pair, and the nucleon  $N_2$  and the nucleus  $A - 2$  recoil with high and low mo-

<sup>a</sup> On leave from Bogoliubov Laboratory of Theoretical Physics, JINR, 141980, Dubna, Moscow reg., Russia

menta, respectively, and are detected in coincidence with the scattered electron. It will be shown that these processes exhibit a series of very interesting features which could in principle provide useful insight on the following basic issues: *i*) the nature and the relevance of FSI in DIS; *ii*) the validity of the spectator mechanism leading to the cross section (9); *iii*) the medium induced modifications of the nucleon structure function; *iv*) the origin of the EMC effect. For the above reasons, the semi-inclusive processes we will consider are worth being theoretically analysed, even though their experimental investigation represents a difficult task. It should be emphasised, in this respect, that the first version of the present paper [8] was motivated by the discussions on the feasibility of an electron-ion collider, where the detection of various nuclear fragments resulting from DIS, could in principle be possible [9,10].

Our paper is organised as follows: in Sect. 2 the basic nuclear quantities which enter the problem, viz. the one-body and two-body nuclear Spectral Functions are briefly discussed; the cross section for the process  $A(e, e'(A-1))X$  is presented in Sect. 3, where the possibilities offered by the process to experimentally check the validity of the spectator mechanism and the properties of the structure function of a mean-field, *weakly bound* nucleon, are discussed; the cross section for the process  $A(e, e'N_2(A-2))X$ , and how this process can be used to investigate the spectator model and the properties of the structure function of a *deeply bound* nucleon, are discussed in Sect. 4; the *local* EMC effect, i.e. the separate contribution to the EMC effect of nucleons having different binding in the nucleus, is discussed in Sect. 5; the Summary and Conclusions are presented in Sect. 6. Appendix A contains the derivation of the cross sections for both processes.

## 2 The nuclear spectral function

In order to make clear the nuclear physics aspects underlying the above processes, few basic concepts about the relationships between the nucleon momentum distributions in the parent nucleus  $A$  and the excitation energy of daughter nuclei  $(A-1)$  and  $(A-2)$  in semi-inclusive processes, will be recalled. The nucleon Spectral Function  $P_{N_1}(|\vec{p}_1|, E)$  represents the joint probability to have in the parent nucleus a nucleon with momentum  $|\vec{p}_1|$  and removal energy  $E$

$$P_{N_1}(|\vec{p}_1|, E) = \langle \Psi_A^0 | a_{\vec{p}_1}^\dagger \delta(E - (H_A - E_A^0)) a_{\vec{p}_1} | \Psi_A^0 \rangle = \sum_f \left| \langle \vec{p}_1, \Psi_{A-1}^f | \Psi_A^0 \rangle \right|^2 \delta(E - (E_{A-1}^f - E_A^0)), \quad (1)$$

where  $a_{\vec{p}_1}^\dagger$  and  $a_{\vec{p}_1}$  are creation and annihilation operators,  $H_A$  is the nuclear Hamiltonian,  $E_A^0$  ( $\Psi_A^0$ ) is the ground state energy (wave function) of  $A$ , and  $E_{A-1}^f = E_{A-1}^0 + E_{A-1}^*$  ( $\Psi_{A-1}^f$ ) is the intrinsic energy (wave function) of  $A-1$ , whose ground state energy is  $E_{A-1}^0$ . Thus, the nucleon removal energy  $E = E_{A-1}^f - E_A^0 = M_{A-1} +$

$M - M_A + E_{A-1}^*$  (where  $M_i$  is the mass of system  $i$ ) is the energy required to remove a nucleon from  $A$  leaving  $(A-1)$  with excitation energy  $E_{A-1}^*$ .

A common representation of the spectral function is as follows (omitting unnecessary here indices and summations) [11]

$$P_{N_1}^A(|\vec{p}_1|, E) = P_0(|\vec{p}_1|, E) + P_1(|\vec{p}_1|, E) \quad (2)$$

where

$$P_0(|\vec{p}_1|, E) = \sum_{\alpha < F} n_\alpha^A(|\vec{p}_1|) \delta(E - \varepsilon_\alpha) \quad (3)$$

and

$$P_1(|\vec{p}_1|, E) = \frac{1}{(2\pi)^3} \frac{1}{2J_0 + 1} \sum_{M_0 \sigma} \sum_{f \neq \alpha} \left| \int d\vec{r} e^{i\vec{p}_1 \cdot \vec{r}} G_{f0}(\vec{r}) \right|^2 \times \delta[E - (E_{A-1}^f - E_A)] \quad (4)$$

In the above equations  $F$  denotes the Fermi level,  $n_\alpha^A(|\vec{p}_1|)$  is the momentum distribution of a bound shell model state with eigenvalue  $\varepsilon_\alpha > 0$ , and  $G_{f0}$  is the overlap between the wave functions of the ground state of the parent  $A$  and the state  $f$  of the daughter  $(A-1)$  (see for details [12–14]). The quantity  $P_0(|\vec{p}_1|, E)$ , represents the shell model contribution to the Spectral Function, where the occupation numbers of the shell model states below the Fermi sea are given by  $N_\alpha = \int d\vec{p}_1 n_\alpha^A(|\vec{p}_1|) < 1$ , whereas  $P_1(|\vec{p}_1|, E)$  provides the contribution from correlations, which deplete the shell model states  $\alpha < F$ . The so called Momentum Sum Rule links the spectral function to the nucleon momentum distribution, viz.

$$n^A(|\vec{p}_1|) = \int_{E_{min}}^{\infty} P_{N_1}^A(|\vec{p}_1|, E) dE = \sum_{\alpha < F} n_\alpha^A(|\vec{p}_1|) + \sum_{f \neq \alpha} \left| \int d\vec{r} e^{i\vec{p}_1 \cdot \vec{r}} G_{f0}(\vec{r}) \right|^2, \quad (5)$$

where  $E_{min} = E_{A-1} - E_A$ . It can therefore be seen that

$$n_0^A(|\vec{p}_1|) \equiv \sum_{\alpha < F} n_\alpha^A(|\vec{p}_1|) = \int_{E_{min}}^{\infty} P_0^A(|\vec{p}_1|, E) dE,$$

represents the momentum distribution in the parent, when the daughter is either in the ground state or in hole states of the parent, whereas

$$n_1^A(|\vec{p}_1|) \equiv n^A(|\vec{p}_1|) - n_0^A(|\vec{p}_1|) = \int_{E_{min}}^{\infty} P_1^A(|\vec{p}_1|, E) dE$$

represents the momentum distribution in the parent, when the daughter is left in highly excited states, with at least one particle in the continuum; this means that  $n_0^A(|\vec{p}_1|)$  is the momentum distribution of weakly bound (shell-model) nucleons, while  $n_1^A(|\vec{p}_1|)$  is the momentum distributions of

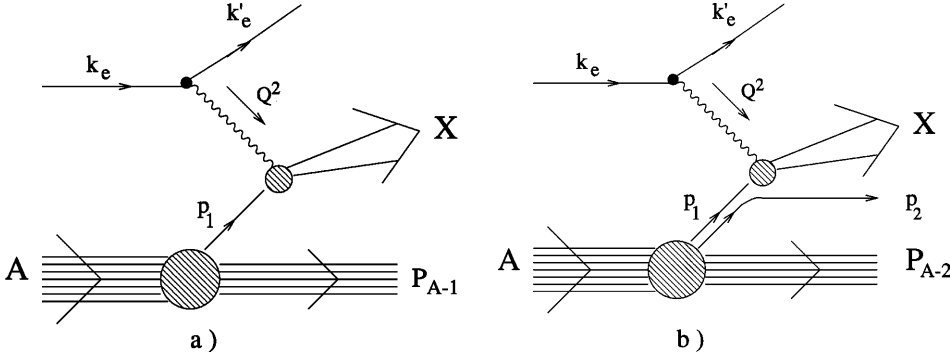


**Fig. 1.** The processes  $A(e, e'(A-1))X$  (a) and  $A(e, e'N_2(A-2))X$  (b) within the Impulse Approximation (the *Spectator mechanism*)

deeply bound nucleons generated by N-N correlations. A realistic model for the latter leads to the following form of the corresponding spectral function  $P_1^A(|\vec{p}_1|, E)$  [12–14]

$$P_1^A(|\vec{p}_1|, E) = \int d^3k_{cm} n_{rel}^A(|\vec{p}_1 - \vec{p}_{cm}/2|) n_{cm}^A(|\vec{p}_{cm}|) \times \delta \left[ E - E_{thr}^{(2)} - \frac{(A-2)}{2M(A-1)} \cdot \left( \vec{p}_1 - \frac{(A-1)\vec{p}_{cm}}{(A-2)} \right)^2 \right], \quad (6)$$

where  $n_{rel}^A$  and  $n_{cm}^A$  are, respectively, the relative and Center of Mass momentum distributions of a correlated pair.

It has been shown [13] that such a model satisfactorily reproduces the nuclear spectral functions calculated within many-body approaches with realistic  $NN$  interaction and describes fairly well the quasi elastic inclusive  $A(e, e')X$  processes.

Within the spectator model, the process  $A(e, e'(A-1))X$  is directly proportional to the one-nucleon spectral function, whereas the process  $A(e, e'N(A-2))X$  is proportional to the two-nucleon spectral function, which is defined as follows

$$P_{N_1N_2}(\vec{p}_2, \vec{p}_1, E^{(2)}) = \langle \Psi_A^0 | a_{\vec{p}_1}^+ a_{\vec{p}_2}^+ \delta(E^{(2)} - (H_{A-2} - E_A)) a_{\vec{p}_2} a_{\vec{p}_1} | \Psi_A^0 \rangle = \sum_f \left| \langle \vec{p}_1, \vec{p}_2, \Psi_{A-2}^f | \Psi_A^0 \rangle \right|^2 \delta(E^{(2)} - (E_{A-2}^f - E_A)), \quad (7)$$

where  $E^{(2)} = E_{th}^{(2)} + E_{A-2}^*$  is the two-nucleon removal energy,  $E_{A-2}^*$  is the intrinsic excitation energy of the  $A-2$  system, and  $E_{th}^{(2)} = 2M + M_{A-2} - M_A$  the two-nucleon break-up threshold. If one adheres to the model leading to (6), the correlated part of the two-nucleon spectral function can be written as follows [5]:

$$P_{N_1N_2}(\vec{p}_1, \vec{p}_2, E^{(2)}) = n_{cm}^A(|\vec{P}_{A-2}|) n_{rel}^A \times (|\vec{p}_2 + \vec{P}_{A-2}/2|) \delta(E^{(2)} - E_{th}^{(2)}) \quad (8)$$

### 3 The $A(e, e'(A-1))X$ process

In Impulse Approximation, the process  $A(e, e'(A-1))X$  (depicted Fig. 1a), represents the absorption of the virtual photon by a quark of a shell-model nucleon, followed by the recoil of the nucleus  $A-1$  in a low momentum,  $\vec{P}_{A-1}$ , and low excitation energy,  $E_{A-1}^*$  state ( $E_{A-1}^* \simeq 0$  or  $\simeq$  shell-model hole state energy of the target); the scattered electron and the nucleus  $(A-1)$  are detected in coincidence. The aim for studying such a process is twofold:

- i) to investigate the nature of the final state interaction (FSI) of the hit quark with the surrounding nuclear medium; as a matter of fact, the observation of a nucleus  $(A-1)$  in the ground state (or in a low shell model excited states) would represent obvious evidence that the leptoproduct hadrons propagated through the nucleus  $(A-1)$  without strong FSI. Therefore, the number of observed  $(A-1)$  systems and its variation with  $A$  could provide important information on e.g. the hadronization length in the medium;
- ii) to investigate the  $A$ -dependence of possible medium induced modifications of the DIS structure function of weakly bound nucleons.

In IA the differential cross section in the laboratory system has the following form (see Appendix A) [8]

$$\sigma_1^A(x_{Bj}, Q^2, \vec{P}_{A-1}) \equiv \sigma_1^A = \frac{d\sigma^A}{dx_{Bj} dQ^2 d\vec{P}_{A-1}} = K^A(x_{Bj}, Q^2, y_A, z_1^{(A)}) z_1^{(A)} \times F_2^{N/A}(x_A, Q^2, p_1^2) n_0^A(|\vec{P}_{A-1}|), \quad (9)$$

where:  $Q^2 = -q^2 = -(k_e - k_e')^2 = \vec{q}^2 - \nu^2 = 4\mathcal{E}_e \mathcal{E}_e' \sin^2 \frac{\theta}{2}$  is the 4-momentum transfer (with  $\vec{q} = \vec{k}_e - \vec{k}_e'$ ,  $\nu = \mathcal{E}_e - \mathcal{E}_e'$  and  $\theta \equiv \theta_{\vec{k}_e \vec{k}_e'}$ );  $x_{Bj} = Q^2/2M\nu$  is the Bjorken scaling

variable;  $p_1 \equiv (p_{10}, \vec{p}_1)$ , with  $\vec{p}_1 \equiv -\vec{P}_{A-1}$ , is the four momentum of the nucleon;  $F_2^{N/A}$  is the DIS structure function of the nucleon  $N$  in the nucleus  $A$ ;  $n_0^A(|\vec{P}_{A-1}|)$  is the 3-momentum distribution of the bound nucleon;  $K^A(x_{Bj}, Q^2, y_A, z_1^{(A)})$  is the following kinematical factor

$$K^A(x_{Bj}, Q^2, y_A, z_1^{(A)}) = \frac{4\alpha^2 \pi}{Q^4 x_{Bj}} \cdot \left(\frac{y}{y_A}\right)^2 \times \left[ \frac{y_A^2}{2} + (1 - y_A) - \frac{p_1^2 x_{Bj}^2 y_A^2}{z_1^{(A)2} Q^2} \right], \quad (10)$$

and

$$y = \nu/\mathcal{E}_e, \quad y_A = (p_1 \cdot q)/(p_1 \cdot k_e) \quad (11)$$

$$x_A = \frac{x_{Bj}}{z_1^{(A)}}, \quad z_1^{(A)} = \frac{p_1 \cdot q}{M\nu}. \quad (12)$$

Nuclear effects in (9) are generated by the nucleon momentum distribution  $n_0^A(|\vec{P}_{A-1}|)$ , and by the quantities  $y_A$  and  $z_1^{(A)}$ , which differ from the corresponding quantities for a free nucleon ( $y = \nu/\mathcal{E}_e$  and  $z_1^{(N)} = 1$ ), if the off mass shellness of the nucleon ( $p_1^2 \neq M^2$ ) generated by nuclear binding is taken into account. Equation (9) is valid for finite values of  $Q^2$ , and for  $A = 2$  agrees with the expression used in [7, 2] (note, that in [7] the quantity  $D^N = K^A/K^N$  has been used,  $K^N$  being the quantity (10) for a free nucleon, which will be discussed later on).

In this paper, we follow the usual procedure consisting of disregarding the explicit dependence of  $F_2^{N/A}$  upon  $p_1^2$ , and choose the form of  $F_2^{N/A}$  to be the same as for the free nucleon; within such an approach, the effect of the nuclear medium will be considered within two main models:

*i) the x-rescaling model*, which directly follows from the convolution formula of inclusive scattering, leading to energy conservation at the hadronic vertex in Fig. 1, i.e.

$$p_{10} = M_A - \sqrt{(M_{A-1} + E_{A-1}^*)^2 + \vec{P}_{A-1}^2}, \quad (13)$$

which, when placed in (11) and (12), leads to the following structure function for a bound nucleon

$$F_2^{N/A}(x_A, Q^2, p_1^2) = F_2^{N/A}\left(\frac{x_{Bj}}{z_1^{(A)}}, Q^2\right) \quad (14)$$

with

$$z_1^{(A)} = (p_{10} + |\vec{P}_{A-1}| \eta \cos \theta_{\vec{P}_{A-1}\vec{q}})/M, \quad (15)$$

and

$$\eta = |\vec{q}|/\nu = \sqrt{1 + \frac{4M^2 x_{Bj}^2}{Q^2}}. \quad (16)$$

Since the  $(A-1)$  system is detected in a low excited state ( $E_{A-1}^* \simeq 0$ ) and with low momentum ( $|\vec{P}_{A-1}| \ll M_{A-1}$ ), (13) can be safely replaced by

$$p_{10} \simeq (M - E_{min}) - \frac{|\vec{P}_{A-1}|^2}{2M_{A-1}}, \quad (17)$$

(15) then becomes

$$z_1^{(A)} \simeq 1 - \frac{E_{min}}{M} - \frac{|\vec{P}_{A-1}|^2}{2MM_{A-1}} + \frac{\eta}{M} |\vec{P}_{A-1}| \cos \theta_{\vec{P}_{A-1}\vec{q}} \quad (18)$$

and for a heavy nucleus, for which the recoil term in (18) is negligibly small, one has

$$z_1^{(A)} \simeq 1 - \frac{E_{min}}{M} + \frac{\eta}{M} |\vec{P}_{A-1}| \cos \theta_{\vec{P}_{A-1}\vec{q}}. \quad (19)$$

Moreover, being  $\frac{E_{min}}{M} \ll 1$ , it can be concluded that the structure functions (14) will exhibit almost no  $A$ -dependent effects, apart from the case of the few nucleon systems ( $A=2,3,4$ ), for which the recoil term in (18) cannot be disregarded. In the Bjorken limit ( $Q^2 \rightarrow \infty$ ,  $\nu \rightarrow \infty$ ,  $x_{Bj} = \text{const}$ ,  $\nu \sim |\vec{q}|$ ),  $\eta \rightarrow 1$ )

$$z_1^{(A)} = (p_{10} + |\vec{P}_{A-1}| \cos \theta_{\vec{P}_{A-1}\vec{q}})/M. \quad (20)$$

Note that (20) can also be written as ( $E_{A-1}^* = 0$  in the processes we are considering)

$$z_1^{(A)} = \frac{M_A}{M} - \frac{M_{A-1} z_{A-1}}{M} \quad (21)$$

where

$$z_{A-1} = \frac{\sqrt{\vec{P}_{A-1}^2 + M_{A-1}^2} - |\vec{P}_{A-1}| \cos \theta_{\vec{P}_{A-1}\vec{q}}}{M_{A-1}} \quad (22)$$

is the light cone momentum of the  $A-1$  recoiling nucleus. (21) is nothing but the energy conservation of the process

$$\nu + M_A = \sqrt{M_X^2 + (\vec{p}_1 + \vec{q})^2} + \sqrt{M_{A-1}^2 + \vec{p}_1^2} \quad (23)$$

in the Bjorken limit, where  $M_X$  is the invariant mass of the produced hadronic state  $X$ ; in the case of the deuteron, the term  $\frac{|E_{min}|}{M}$  can be disregarded, so that  $M_A/M \simeq 2$  and the well known relation  $z_1^{(2)} = 2 - z_2$ , where  $z_2 = (\sqrt{|\vec{p}_2|^2 + M^2} - |\vec{p}_2| \cos \theta_{\vec{p}_2\vec{q}})/M$ , and  $\vec{p}_2$  is the momentum of the recoiling nucleon, is recovered.

*ii) the  $Q^2$ -rescaling model* [15], which is based on the idea of a medium modification of the  $Q^2$ -evolution equations of  $QCD$ , leading to

$$F_2^{N/A}(x, Q^2) = F_2^N(x, \xi_A(Q^2)Q^2), \quad (24)$$

where the  $Q^2$  dependence of the quantity  $\xi_A(Q^2)$  is determined so as to satisfy the  $QCD$  evolution equations on both sides of (24), with the additional hypothesis that the quark confinement radius for a bound nucleon ( $\lambda_A$ ) is larger than that for a free nucleon ( $\lambda_N$ ), according to the ansatz

$$\frac{\lambda_A^2}{\lambda_N^2} = \frac{\mu_N^2}{\mu_A^2} = \xi_A(\mu_A^2), \quad (25)$$

where  $\mu_A$  and  $\mu_N$  are the lower momentum cutoffs for the bound and free nucleons, respectively. The following relation can then be obtained

$$\xi_A(Q^2) = \left( \frac{\lambda_A^2}{\lambda_N^2} \right)^{\frac{\ln(Q^2/\Lambda_{QCD}^2)}{\ln(\mu_A^2/\Lambda_{QCD}^2)}}, \quad (26)$$

where  $\Lambda_{QCD}$  is the universal  $QCD$  scale parameter.

To sum up, in the  $Q^2$ -rescaling model an explicit  $A$  dependence is provided by (26) whereas, in the  $x$ -rescaling model, the  $A$ -dependence of  $F_2^{N/A}$  is generated implicitly by the momentum  $|\vec{P}_{A-1}|$  of the detected  $A-1$  system (cf. (18)).

We will now discuss a series of processes, which could in principle provide useful insight on the following basic issues: *i*) the nature and the relevance of FSI in DIS; *ii*) the validity of the spectator mechanism leading to the cross section (9); *iii*) the medium induced modifications of the nucleon structure function; *iv*) the origin of the *EMC* effect.

### 3.1 Checking the spectator mechanism in the semi-inclusive process $A(e, e'(A-1))X$

The validity of the spectator mechanism could experimentally be checked in the following way. Let us consider the cross section (9) for two different nuclei  $A$  and  $A'$ , and the same values of  $x_{Bj}$ ,  $Q^2$  and  $|\vec{P}_{A-1}| = |\vec{P}_{A'-1}|$ . Consider now the ratio

$$\begin{aligned} R(x_{Bj}, Q^2, |\vec{P}_{A-1}|, z_1^{(A)}, z_1^{(A')}, y_A, y_{A'}) \\ &= \frac{\sigma_1^A(x_{Bj}, Q^2, |\vec{P}_{A-1}|, z_1^{(A)}, y_A)}{\sigma_1^{A'}(x_{Bj}, Q^2, |\vec{P}_{A-1}|, z_1^{(A')}, y_{A'})} \\ &= \frac{K^A}{K^{A'}} \frac{z_1^{(A)} F_2^{N/A}(x_A, Q^2, p_1^2)}{z_1^{(A')} F_2^{N/A'}(x_{A'}, Q^2, p_1^2)} \frac{n_0^A(|\vec{P}_{A-1}|)}{n_0^{A'}(|\vec{P}_{A-1}|)}, \quad (27) \end{aligned}$$

with  $y_A$  and  $z_1^{(A)}$  defined in (11) and (12), respectively. For reasons that would be clear later on, our aim is to get rid as much as possible of the various  $A$  and  $A'$  dependencies appearing in (27), except the ones provided by the nucleon momentum distributions. The dependence upon  $A$  and  $A'$  is contained in the quantities  $z_1^{(A)}$ ,  $x_A$ ,  $K^A$ , and  $n_0^A(|\vec{P}_{A-1}|)$ ; in order to get rid of the  $A$ -dependence due to the first three quantities let us consider coplanar kinematics, i.e.

$$y_A = y \cdot \frac{p_{10} + \eta |\vec{P}_{A-1}| \cos \theta_{\vec{P}_{A-1}\vec{q}}}{p_{10} + \eta |\vec{P}_{A-1}| \cos \theta_{\vec{P}_{A-1}\vec{k}_e}}, \quad (28)$$

with

$$\begin{aligned} \cos \theta_{\vec{P}_{A-1}\vec{q}} &= -\cos(\theta_{\vec{P}_{A-1}\vec{k}_e} + \theta_{\vec{q}\vec{k}_e}); \\ \cos \theta_{\vec{q}\vec{k}_e} &= \left( 1 + \frac{Mx_{Bj}}{\mathcal{E}_k} \right) / \eta. \quad (29) \end{aligned}$$

In the Bjorken limit  $\eta \rightarrow 1$ ,  $z_1^{(A)} = (p_{10} + |\vec{P}_{A-1}| \cos \theta_{\vec{P}_{A-1}\vec{q}}) / M$  (cf. (15)),  $\theta_{\vec{P}_{A-1}\vec{q}} \rightarrow \theta_{\vec{P}_{A-1}\vec{k}_e}$ ,  $y_A \rightarrow y$ , and

$$\begin{aligned} K^A(x_{Bj}, Q^2, y_A, z_1^{(A)}) &\rightarrow K^N(x_{Bj}, Q^2, y) \\ &= \frac{4\alpha^2}{Q^4} \frac{\pi}{x_{Bj}} \cdot \left[ \frac{y^2}{2} + 1 - y - \frac{Q^2}{4\mathcal{E}_e^2} \right], \quad (30) \end{aligned}$$

where  $K^N$  is nothing but the trivial kinematic factor appearing in the DIS  $eN$ - inclusive cross section; the cross section (9) thus becomes

$$\begin{aligned} \left( \frac{d\sigma^A}{dx_{Bj} dQ^2 d\vec{P}_{A-1}} \right)_{Bj} &= K^N(x_{Bj}, Q^2, y) z_1^{(A)} \\ &\times F_2^{N/A}(x_{Bj}/z_1^{(A)}, Q^2) n_0^A(|\vec{P}_{A-1}|), \quad (31) \end{aligned}$$

with the  $A$ -dependence now appearing only in  $F_2^{N/A}$ ,  $n_0^A(|\vec{P}_{A-1}|)$  and  $z_1^{(A)}$ . The latter dependence, however, can be eliminated by considering that (18) reduces (due to  $E_{min}/M \ll 1$ ) to  $z_1^{(A)} \simeq 1 - \frac{|\vec{P}_{A-1}|^2}{2MM_{A-1}} + \frac{|\vec{P}_{A-1}|}{M} \cos \theta_{\vec{P}_{A-1}\vec{q}}$ , so that by fixing  $|\vec{P}_{A-1}|$ , and properly changing  $\theta_{\vec{P}_{A-1}\vec{q}}$ , the condition  $z_1^{(A)} \sim z_1^{(A')}$  can easily be achieved. As a result, the Bjorken limit of (27) becomes

$$\begin{aligned} R_{Bj}(x_{Bj}/z_1^{(A)}, Q^2, |\vec{P}_{A-1}|, A, A') \\ &= \frac{F_2^{N/A}(x_{Bj}/z_1^{(A)}, Q^2) n_0^A(|\vec{P}_{A-1}|)}{F_2^{N/A'}(x_{Bj}/z_1^{(A')}, Q^2) n_0^{A'}(|\vec{P}_{A-1}|)} \\ &\rightarrow \frac{n_0^A(|\vec{P}_{A-1}|)}{n_0^{A'}(|\vec{P}_{A-1}|)} \equiv R(|\vec{P}_{A-1}|), \quad (32) \end{aligned}$$

where the last step is strictly valid only within the  $x$ -rescaling model, for in the  $Q^2$ -rescaling model the additional  $A$  and  $A'$ -dependences appearing in  $F_2^{N/A}(x, Q^2) = F_2^N(x, \xi_A(Q^2)Q^2)$  does not cancel out, being different in the numerator and the denominator; such a dependence, however, is overwhelmed by the  $A$ -dependence of  $n_0(|\vec{P}_{A-1}|)$  as it will be shown later on.

We have thus obtained that in the Bjorken limit the  $A$  dependence of the ratio  $R$  is entirely governed by the  $A$  dependence of the nucleon momentum distribution  $n_0^A(|\vec{P}_{A-1}|)$ . Since the latter exhibits a strong  $A$  dependence for low values of  $|\vec{P}_{A-1}|$ , a plot of  $R$  versus  $|\vec{P}_{A-1}|$  should reproduce the behaviour of  $n_0^A(|\vec{P}_{A-1}|)$  which is fairly well known, so that the experimental observation of such a behaviour would represent a stringent test of the spectator mechanism independently of the model for  $F_2^{N/A}$ .

Figure 2 illustrates the expected behaviour of the ratio (32) for  $A = 2$  and different values of  $A'$ . The measurement of the quantity  $R$  shown in Fig. 2 would imply the detection, in coincidence with scattered electrons, of backward recoiling, with momentum  $\vec{P}_{A-1}$ , protons, deuterons,  ${}^3\text{He}$  and  ${}^{12}\text{C}$  nuclei resulting from the

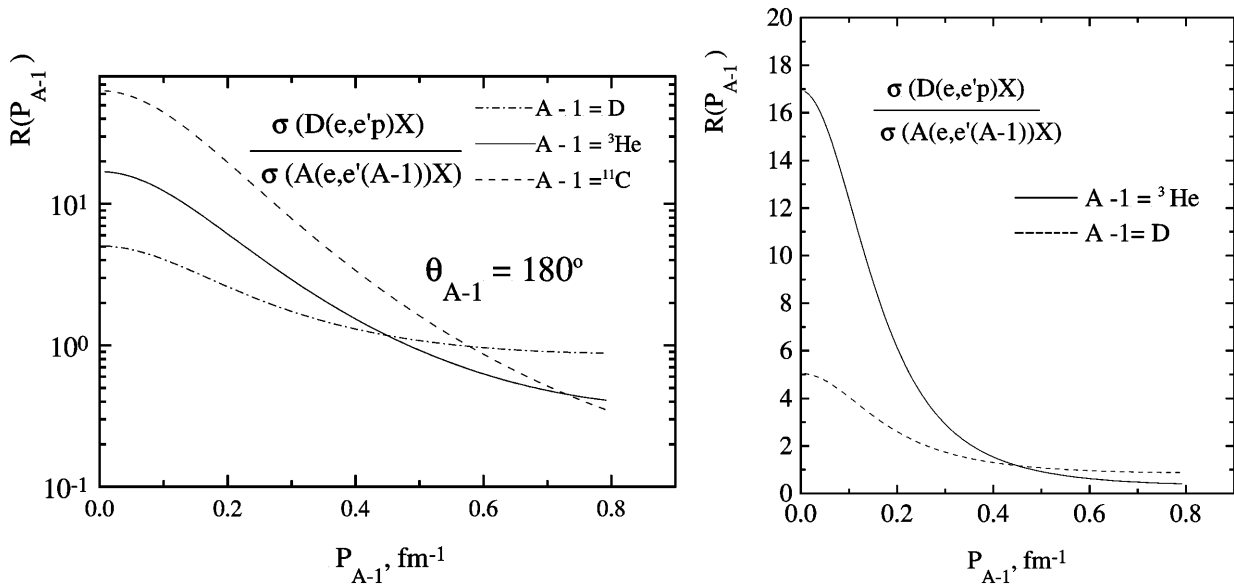


**Fig. 2.** (a) The ratio  $R(|\vec{P}_{A-1}|) = \frac{\sigma[D(e,e'p)X]}{\sigma[A(e,e'(A-1))X]}$  (32) for different nuclei  $A$ , viz  ${}^3\text{H}$ ,  ${}^4\text{He}$  and  ${}^{12}\text{C}$ , assuming that DIS took place on a neutron. The ratio is plotted versus the value of the targets  $P_{A-1} \equiv |\vec{P}_{A-1}| = |\vec{P}_{A'-1}|$  of the nucleus emitted backward. (b) The same as in (a) but on a linear plot for the targets  ${}^3\text{H}$  and  ${}^4\text{He}$  (in this and in the following Figures  $\theta_{P_{A-1}} \equiv \theta_{\widehat{\vec{P}_{A-1}\vec{q}}}$ )

processes  $D(e, e'p)X$ ,  ${}^3\text{H}(e, e'D)X$ ,  ${}^4\text{He}(e, e'{}^3\text{He})X$  and  ${}^{12}\text{C}(e, e'{}^{11}\text{C})X$ , respectively, with the DIS scattering processes supposed to occur on a neutron.<sup>1</sup> Since the results presented in Fig. 2 were obtained in the Bjorken limit, where  $K^A = K^{A'} = K^N$ , let us analyse at which value of  $Q^2$  such an equality is fulfilled. To this end, in Fig. 3 the ratio  $K^A/K^N$  is shown vs.  $Q^2$  for of  $A = 4$ . It can be seen that at  $Q^2 \simeq 5\text{GeV}^2$   $K^A$  and  $K^N$  differ by 5% only. The cross sections corresponding to the processes considered in Fig. 2 are presented in Fig. 4.

From the results we have exhibited, it is clear that the observation of recoiling nuclei in the ground state, with a  $|\vec{P}_{A-1}|$ -dependence similar to the one predicted by the momentum distributions, would represent a stringent check of the spectator mechanism, which, in turns, would indicate the absence of significant FSI between the lepto-produced hadronic states and the nuclear medium. The experimental observation of  $(A - 1)$  nuclei in the ground states would represent a strong indication that the hadronization length is larger than the effective nuclear dimension, since if the hit quark hadronizes inside the nucleus, the latter is expected to be strongly excited. Of particular relevance, in this respect, would be the processes  ${}^3\text{He}({}^3\text{H})(e, e'D)X$ , for if FSI plays an important role, the weakly bound final state deuteron will easily break down. It is clear, therefore, that the experimental observation of

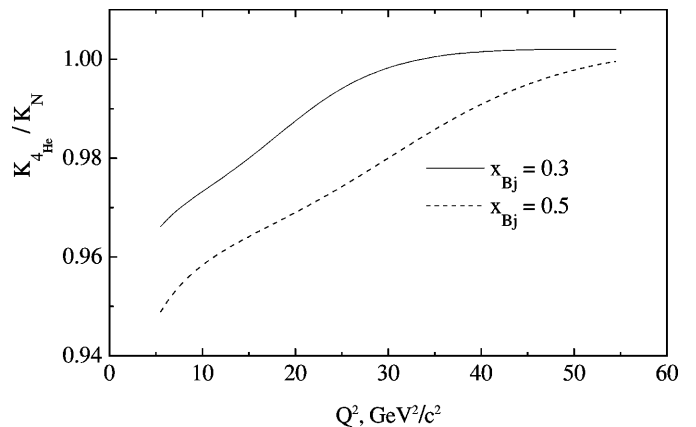


**Fig. 3.** The ratio of the kinematical factor  $K^A(x_{Bj}, Q^2, y_A, z_1^{(A)})$ , (10), for  ${}^4\text{He}$ , to the same quantity for a free nucleon  $K^N(x_{Bj}, Q^2, y)$ , (30), vs.  $Q^2$  for two values of  $x_{Bj}$

<sup>1</sup> Note that the condition  $z_1^{(A)}/z_1^{(A')} = 1$  cannot be achieved if both  $\theta_{\widehat{\vec{P}_{A-1}\vec{q}}}$  are fixed, so that in Fig. 2  $z_1^{(A)}/z_1^{(A')}$  is a function of  $P_{A-1}$ ; however the  $P_{A-1}$ -dependence of the quantity  $z_1^{(A)}F_2^{N/A}(x_{Bj}/z_1^{(A)})/z_1^{(A')}F_2^{N/A'}(x_{Bj}/z_1^{(A)})$  is at most of the order 5 percents and the dependence of  $R(|\vec{P}_{A-1}|)$  upon  $|\vec{P}_{A-1}|$  is entirely provided by the momentum distributions.

the exclusive process  $A(e, e'(A-1)_{gr})X$  is strong evidence of the smallness of FSI. Although recent calculations [16] and experimental data [17] seem to indicate that FSI on a complex nucleus are small in semi inclusive DIS, particularly when the low momentum hadrons are detected backward, the situation is not clearly settled, and therefore the observation of protons and deuterons emitted backward in the processes  $D(e, e'p)X$ ,  ${}^3\text{He}(e, e'D)X$  with a  $|\vec{P}_{A-1}|$  dependence shown in Fig. 2, would represent strong indication of the absence of FSI. The situation here is different from the usually investigated semi-inclusive DIS processes  $A(e, e'N)X$  where the detected nucleon can originate not only from a correlated pair, as originally suggested [2],

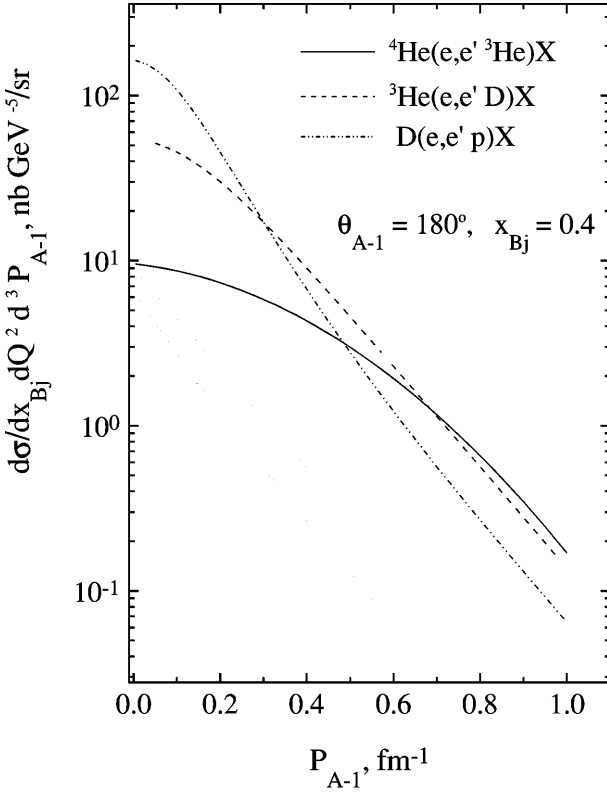


**Fig. 4.** The cross section for the process  $A(e, e'(A-1))X$ , (9) on different targets with the nucleus  $(A-1)$  emitted backward with momentum  $P_{A-1} \equiv |\vec{P}_{A-1}|$

but from competitive processes as well, such as nucleon current and target fragmentations [4,5].

Let us now discuss the possibility to obtain information on the nucleon structure function of a weakly bound nucleon by means of the process  $A(e, e'(A-1))X$ .

### 3.2 Investigating the structure functions of weakly bound nucleons by the process $A(e, e'(A-1))X$

Consider the following quantity

$$R^A(x_{Bj}, x'_{Bj}, Q^2, |\vec{P}_{A-1}|) \equiv \frac{\sigma_1^A(x_{Bj}, Q^2, |\vec{P}_{A-1}|, z_1^{(A)}, y_A)}{\sigma_1^A(x'_{Bj}, Q^2, |\vec{P}_{A-1}|, z_1^{(A)}, y_A)} \quad (33)$$

which represents the ratio between the cross section (9) on the nucleus  $A$  considered at two different values of the Bjorken scaling variable. It is clear that all terms of (9), but the nucleon structure functions, cancel out in the ratio, and one has

$$R^A(x_{Bj}, x'_{Bj}, z_1^{(A)}, Q^2) = \frac{x'_{Bj} F_2^{N/A} \left( \frac{x_{Bj}}{z_1^{(A)}}, Q^2 \right)}{x_{Bj} F_2^{N/A} \left( \frac{x'_{Bj}}{z_1^{(A)}}, Q^2 \right)} \quad (34)$$

in the  $x$ -rescaling approach, and

$$R^A(x_{Bj}, x'_{Bj}, Q^2) = \frac{x'_{Bj} F_2^{N/A} (x_{Bj}, \xi_A(Q^2)Q^2)}{x_{Bj} F_2^{N/A} (x'_{Bj}, \xi_A(Q^2)Q^2)} = \text{constant}, \quad (35)$$

in the  $Q^2$ -rescaling model. (34) and (35) will in general exhibit a different  $|\vec{P}_{A-1}|$  dependence: (35) will be a  $|\vec{P}_{A-1}|$ -independent constant different for different nuclei, whereas (34) will depend both upon  $A$  and  $|\vec{P}_{A-1}|$ , due to the dependence of  $z_1^{(A)}$  upon  $|\vec{P}_{A-1}|$  (cf. (15) with  $\eta = 1$ ). Let us consider the ratio (33) for the deuteron and for a complex nucleus; placing (17) in (15), one obtains  $z_1^{(2)} \simeq 1 - \frac{\varepsilon_D}{M} - \frac{|\vec{P}_{A-1}|^2}{2M^2} + \frac{|\vec{P}_{A-1}|}{M} \cos \theta_{\vec{P}_{A-1}\vec{q}}$  and a strong  $|\vec{P}_{A-1}|$  dependence will originate from the recoil and the angle-dependent terms; for a complex nucleus; one gets  $z_1^{(A)} \simeq 1 - \frac{E_{min}}{M} + \frac{|\vec{P}_{A-1}|}{M} \cos \theta_{\vec{P}_{A-1}\vec{q}}$ , which appreciably differs from unity only for  $\theta_{\vec{P}_{A-1}\vec{q}} = 180^\circ$  and/or large values of  $|\vec{P}_{A-1}|$ . Thus, the  $|\vec{P}_{A-1}|$ -dependence of the ratio (34) can be changed by varying the dependence of  $z_1^{(A)}$  upon  $|\vec{P}_{A-1}|$ ; in such a way,  $\frac{x_{Bj}}{z_1^{(A)}} \neq \frac{x'_{Bj}}{z_1^{(A)}}$  and  $R^A$  will differ from a constant. The ratio (34), for  $A = 2$  and  $A = 40$ , is shown in Figs. 5 and 6 in correspondence of two values of the emission angle  $\theta_{\vec{P}_{A-1}\vec{q}}$  of the nucleus  $A-1$  ( $\theta_{\vec{P}_{A-1}\vec{q}} = 90^\circ$  and  $180^\circ$ ), and  $x_{Bj} = 0.2$  and  $x'_{Bj} = 0.5$ . It can indeed be seen that: *i*) in the  $Q^2$ -rescaling model the ratio is independent of  $|\vec{P}_{A-1}|$ , *ii*) when  $\theta_{\vec{P}_{A-1}\vec{q}} = 90^\circ$ , the  $x$ -rescaling model predicts a  $|\vec{P}_{A-1}|$ -independent ratio for  ${}^{40}\text{Ca}$  ( $z_1^{(40)} \simeq 1$ ) and a strongly  $|\vec{P}_{A-1}|$ -dependent ratio for  $D$  ( $z_1^{(2)} \simeq 1 - \frac{|\vec{P}_{A-1}|^2}{2M^2}$ ); when  $\theta_{\vec{P}_{A-1}\vec{q}} = 180^\circ$ , also the ratio for  ${}^{40}\text{Ca}$  becomes strongly  $|\vec{P}_{A-1}|$ -dependent, for, now,  $z_1^{(40)} \simeq 1 - \frac{|\vec{P}_{A-1}|}{M}$ . To sum up, it can be seen that the semi-inclusive process allows one to choose a variety of kinematical conditions which enhance various aspects of the problem. We have seen in Sect. 3.2 that, due to the small values of  $|\vec{P}_{A-1}|$  and  $E_{min}$ , the process  $A(e, e'(A-1))X$  on a complex nucleus is characterized by  $z_1^{(A)} \simeq 1$  when  $\theta_{\vec{P}_{A-1}\vec{q}} = 90^\circ$ ; as a result, the off-mass-shell dependence of  $F_2^{N/A}$  disappears (cf. full curve in Fig. 5); the off-mass-shell dependence of  $F_2^{N/A}$  can on the contrary be enhanced if  $\theta_{\vec{P}_{A-1}\vec{q}} = 180^\circ$ , for an appreciable contribution from the last term of (18) is now generated; if so, however, the ratio (34) for a complex nucleus will not appreciably differ from that of the deuteron (cf. full curves in Fig. 6), since off-mass-shell effects are solely due to the nucleon momentum  $|\vec{P}_{A-1}|$ , and not to medium effects provided by e.g. the nucleon binding ( $E_{min}/M \ll 1$ ). Possible modifications of  $F_2^{N/A}$  due to medium effects, will be discussed in the next Section.

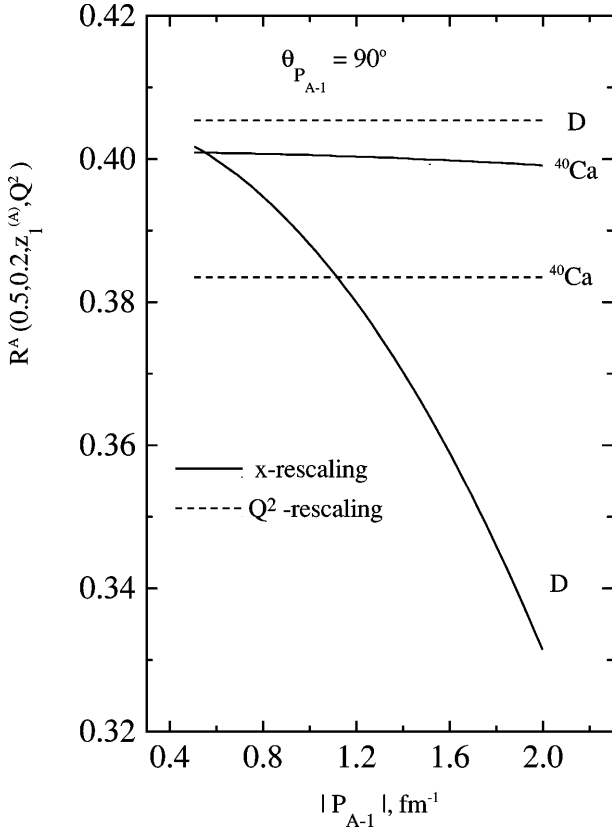


**Fig. 5.** The ratio  $R^A(x_{Bj}, x'_{Bj}, z_1^{(A)}, Q^2)$  (33) for  $A = 2$  and  $A = 40$ ,  $x_{Bj} = 0.2$  and  $x'_{Bj} = 0.5$ ,  $Q^2 = 20 \text{ GeV}^2/c^2$ , plotted versus the momentum of the nucleus  $(A - 1)$  emitted at  $90^\circ$ . The full and dashed curves were obtained within the binding (x-rescaling) and  $Q^2$ -rescaling models, respectively

#### 4 The $A(e, e'N_2(A - 2))X$ process

In the previous Section we have discussed the case of weakly bound, non-correlated nucleons. In the present section we will investigate the semi inclusive processes occurring on a strongly correlated nucleon pair. To this end, let us consider the process depicted in Fig. 1 (b), which represents the absorption of the virtual photon by a correlated nucleon  $N_1$  (with high momentum  $|\vec{P}_{A-1}|$ ), followed by the emission of the partner nucleon  $N_2$  (with momentum  $\vec{p}_2$ ), and by the recoil of the  $(A - 2)$  system, with low momentum  $\vec{P}_{A-2} = -(\vec{P}_{A-1} + \vec{p}_2)$  and low excitation energy. The experimental investigation of such a process would require the coincidence detection of the scattered electron, the nucleon  $N_2$  and the system  $(A - 2)$ .

The differential cross section of the process reads as follows

$$\sigma_2^A(x_{Bj}, Q^2, \vec{P}_{A-2}, \vec{p}_2) \equiv \frac{d\sigma^A}{dx_2 dQ^2 d\vec{P}_{A-2} d\vec{p}_2} = \frac{K^A(x_{Bj}, Q^2, y_A, z_1^{(A)}) z_1^{(A)} F_2^{N/A}(x_{Bj}/z_1^{(A)}, Q^2)}{n_{cm}^A(|\vec{P}_{A-2}|) n_{rel}^A(|\vec{p}_2 + \vec{P}_{A-2}/2|)} \quad (36)$$

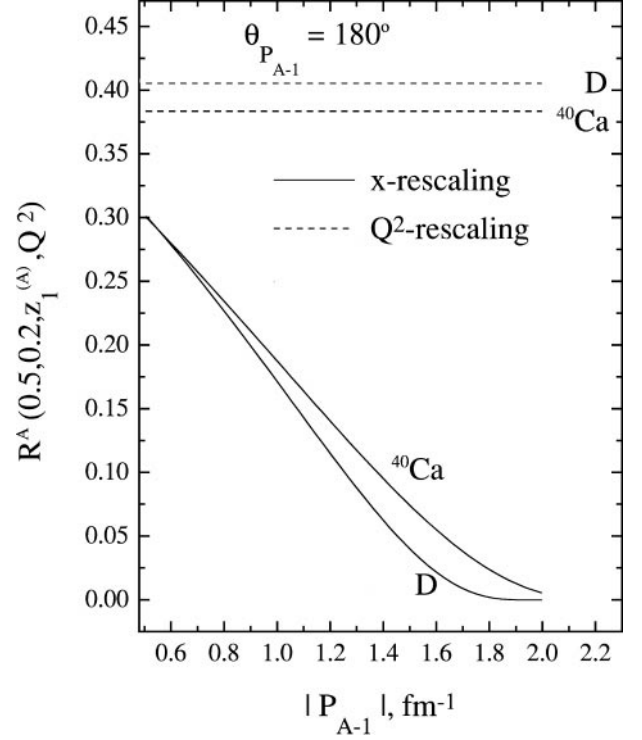


**Fig. 6.** The same as in Fig. 5 for nuclei  $(A - 1)$  emitted backward

where  $P_{N_1, N_2}$  is the two-nucleon spectral function, defined in Section II, and  $K^A$ ,  $y$ ,  $y^A$ ,  $x^A$ , and  $z_1^A$  are defined by (10), (11), (12), and (15) with

$$\vec{p}_1 = -\vec{P}_{A-1} = (\vec{p}_2 + \vec{P}_{A-2}) . \quad (37)$$

and

$$p_{10} = M_A - \sqrt{M^2 + \vec{p}_2^2} - \sqrt{M_{A-2}^2 + \vec{P}_{A-2}^2} . \quad (38)$$

In the Bjorken limit  $\eta = 1$  one has

$$z_1^{(A)} = \frac{M_A}{M} - z_2 - \frac{M_{A-2}}{M} z_{A-2}, \quad (39)$$

where

$$z_2 = \frac{\sqrt{M^2 + \vec{p}_2^2} - |\vec{p}_2| \cos \theta_{\vec{p}_2 \vec{q}}}{M} \quad (40)$$

and

$$z_{A-2} = \frac{\sqrt{M_{A-2}^2 + \vec{P}_{A-2}^2} - |\vec{P}_{A-2}| \cos \theta_{\vec{P}_{A-2} \vec{q}}}{M_{A-2}} \quad (41)$$

are the light cone momentum fraction of nucleon  $N_2$  and nucleus  $(A - 2)$ , respectively. Note that (39) is nothing but the energy conservation of the process

$$\nu + M_A = \sqrt{M_x^2 + (\vec{p}_1 + \vec{q})^2} + \sqrt{M^2 + \vec{p}_2^2} + \sqrt{M_{A-2}^2 + \vec{P}_{A-2}^2} \quad (42)$$



in the Bjorken limit. In the non relativistic approximation one obtains

$$z_1^{(A)} \simeq 1 - \frac{E}{M} - \frac{|\vec{P}_{A-1}|^2}{2(A-1)M^2} + \frac{|\vec{P}_{A-1}|}{M} \cos\theta_{\widehat{\vec{p}_2 \vec{P}_{A-1}}}, \quad (43)$$

with  $E = (E_{th}^{(2)} + E_{A-1}^*)$ . Due to the small value of  $\vec{k}_{cm} = -\vec{P}_{A-2}$ , we can write  $E_{A-1}^* \simeq \frac{(A-2)}{2M(A-1)} |\vec{P}_{A-1}|^2$ , and by considering that  $\vec{P}_{A-1} = -(\vec{p}_2 + \vec{P}_{A-2})$  (cf. (37)), one gets:

$$E = E_{th}^{(2)} + \frac{(A-2)}{2M(A-1)} \left[ |\vec{p}_2|^2 + \left( \frac{A-1}{A-2} \right)^2 \vec{P}_{A-2}^2 + 2 \frac{A-1}{A-2} |\vec{p}_2| |\vec{P}_{A-2}| \cos\theta_{\widehat{\vec{p}_2 \vec{P}_{A-2}}} \right]. \quad (44)$$

It should be stressed that the nucleon structure function  $F_2^{N/A}(x_{Bj}/z_1^{(A)}, Q^2)$  appearing in (9) and (36) reflects different physical situations, for in the first case  $F_2^{N/A}$  represents the quark distribution in a weakly bound, quasi-free nucleon, whereas, in the second case, it represents the quark distribution in a strongly bound nucleon, which, in principle, can undergo, because of binding, off-mass-shell deformations (see, for instance [18,19]). Therefore, if the nucleon structure function could be extracted from the cross section (36) and compared with the one obtained from the cross section (9), a direct comparison of nucleon structure functions for weakly bound and deeply bound nucleons could, for the first time, be carried out.

It should be pointed out that, since  $y_A$  depends upon the high momentum  $|\vec{p}_2|$ , the factor  $K^A(x_{Bj}, Q^2, y_A)$  may strongly differ from  $K^N(x_{Bj}, Q^2, y)$ , unless one of the two following kinematical conditions are chosen: *i*) small values of  $x_{Bj}$ ; *ii*) the Bjorken limit. We found that at  $Q^2 = 20 \text{ GeV}^2/c^2$  and  $x_{Bj} = 0.05$ , the direction of the momentum transfer  $\vec{q}$  coincides, in the frame where the target is at rest, with the electron beam direction ( $\theta_{\widehat{\vec{k} \vec{q}}} \approx 2^0$ ); in this case,  $y_A \simeq y$  and  $K^A \simeq K^N$  (our numerical estimates show that  $K^A/K^N$  varies from 0.99 at  $|\vec{p}_2| = 350 \text{ MeV}/c$  to 0.96 at  $|\vec{p}_2| = 1 \text{ GeV}/c$ ); adopting realistic figures for an electron-ion collider, i.e.  $\mathcal{E}_e \approx 5 \text{ GeV}$ ,  $T_N = (\text{kinetic energy per nucleon}) \approx 25 \text{ GeV}$  [10] in its laboratory system, the chosen values of  $Q^2$  and  $x_{Bj}$  correspond to  $\mathcal{E}'_e \approx 2 \text{ GeV}$ ;  $\theta_{\widehat{\vec{k} \vec{k}'}} \approx 90^0$  (in the nucleus rest frame they would correspond to  $\mathcal{E}_e \approx 260 \text{ GeV}$ ,  $\mathcal{E}'_e \approx 50 \text{ GeV}$ ;  $\theta_{\widehat{\vec{k} \vec{k}'}} \approx 2^0$ ).

#### 4.1 Checking the spectator mechanism in the semi-inclusive process $A(e, e' N_2(A-2))X$

The validity of (36) can experimentally be tested by taking advantage of the observation [20] that for high values of  $|\vec{P}_{A-1}|$  the nucleon momentum distribution for a complex nucleus turns out to be the rescaled momentum distribution of the deuteron, with very small  $A$  dependence (unlike what happens for the low momentum part of  $n(k)$

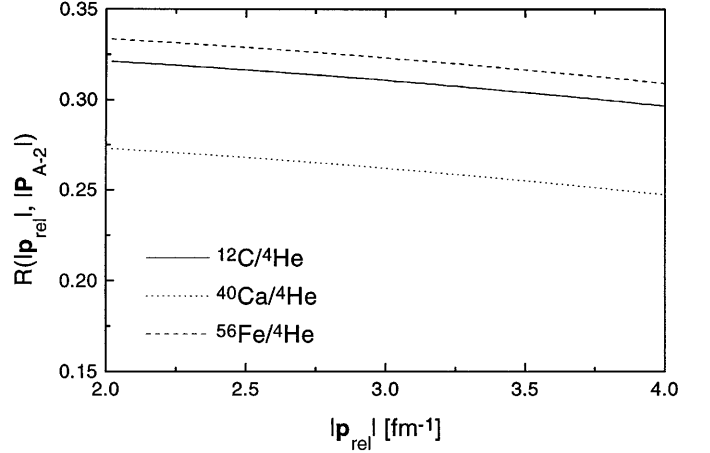


**Fig. 7.** The ratio (45), calculated at  $Q^2 = 20 \text{ GeV}^2/c^2$ ,  $|\vec{P}_{A-2}| = |\vec{P}_{A'-2}| = 50 \text{ MeV}/c$ ,  $x_{Bj} = 0.4$ ,  $\theta_{\widehat{\vec{p}_2 \vec{P}_{A-2}}} = \theta_{\widehat{\vec{p}_2 \vec{P}_{A'-2}}} = 10^0$ , for  $A = 12, 40$  and  $56$  and  $A' = 4$ , versus  $|\vec{p}_{rel}| = |\vec{p}_2 + \vec{P}_{A-2}|$  ( $|\vec{p}_2|$  is varied)

(cf. Fig. 2)). Let us therefore consider the following ratio, where  $|\vec{P}_{A-2}| = |\vec{P}_{A'-2}|$ :

$$\begin{aligned} R(x_{Bj}, Q^2, \vec{P}_{A-2}, \vec{p}_2, z_1^{(A)}, z_1^{(A')}) & \\ & \equiv \frac{\sigma_2^A(x_{Bj}, Q^2, \vec{P}_{A-2}, |\vec{p}_2|)}{\sigma_2^{A'}(x_{Bj}, Q^2, \vec{P}_{A-2}, |\vec{p}_2|)} \\ & = \frac{z_1^{(A)} F_2^{N/A}(x_{Bj}/z_1^{(A)}, Q^2)}{z_1^{(A')} F_2^{N/A'}(x_{Bj}/z_1^{(A')}, Q^2)} \\ & \cdot \frac{n_{rel}^A(|\vec{p}_{rel}|)}{n_{rel}^{A'}(|\vec{p}_{rel}|)} \cdot \frac{n_{cm}^A(|\vec{P}_{A-2}|)}{n_{cm}^{A'}(|\vec{P}_{A-2}|)}, \end{aligned} \quad (45)$$

where  $|\vec{p}_{rel}| = |\vec{p}_2 + \vec{P}_{A-2}|/2$ . If  $|\vec{P}_{A-2}|$  is fixed, then, provided  $F_2^{N/A} = F_2^{N/A'}$ , the ratio, measured at  $p_{rel} \geq 2 - 3 \text{ fm}^{-1}$ , would be roughly a constant, since  $n_{rel}^A \propto n^D$  for any  $A$ . The condition  $F_2^{N/A} = F_2^{N/A'}$  can be achieved by properly choosing, for  $A$  and  $A'$ , the values of  $\vec{p}_2$  and  $\vec{P}_{A-2}$  appearing in (44), so as to make  $z_1^{(A)} \simeq z_1^{(A')}$ , i.e.  $F_2^{N/A} \simeq F_2^{N/A'}$  (note, moreover, that for large values of  $|\vec{P}_{A-1}|$  and large values of  $A$ , the dependence of  $z_1^{(A)}$  upon  $A$  is unessential). To summarize, the cross-section (36) should be measured for the systems  $A$  and  $A'$  at the same values of  $x_{Bj}$ ,  $Q^2$  and  $\vec{P}_{A-2}$ , changing the values of the angle  $\theta_{\widehat{\vec{p}_2 \vec{P}_{A-2}}}$  and  $|\vec{p}_2|$  so as to vary  $|\vec{p}_{rel}| = |\vec{p}_2 + \vec{P}_{A-2}|/2$ , keeping  $z_1^{(A)} = z_1^{(A')}$ . If (36) is basically correct, the ratio (45) plotted versus  $|\vec{p}_{rel}| \geq 2 - 3 \text{ fm}^{-1}$  should exhibit (as shown in Fig. 7) the same deuteron-like behaviour for any two nuclei in the range, say,  $2 < A < 208$ . If such a deuteron-like behaviour of (45) is experimentally found, it would represent a stringent test of the spectator mechanism. A word of caution is however in order here: the FSI between the nucleon  $N_2$  and the nucleus  $(A-2)$  will presumably affect the ratio (45). Calculations of the FSI

within the Glauber multiple scattering approach are in progress and will be reported elsewhere; preliminary results indicate that in the region of the considered kinematics, the replacement of the undistorted two-body Spectral Function with the distorted one, mainly affects the absolute value of the ratio (45).

#### 4.2 Investigating the structure functions of deeply bound nucleons by the process $A(e, e'N_2(A-2))X$

As in the case of the  $A(e, e'(A-1))X$  process, in order to investigate the structure function of a (deeply) bound nucleon, we have to figure out experimentally measurable quantities which could provide information on  $F_2^{N/A}$  without contaminations from the nucleon momentum distributions, or other momentum dependent terms. To this end, we use the analog of the ratio (33) which, within the convolution model, assumes the following form

$$R(x_{Bj}, x'_{Bj}, Q^2, |\vec{P}_{A-2}|, |\vec{p}_2|) \equiv \frac{\sigma_2^A(x_{Bj}, Q^2, |\vec{P}_{A-2}|, |\vec{p}_2|)}{\sigma_2^A(x'_{Bj}, Q^2, |\vec{P}_{A-2}|, |\vec{p}_2|)} \\ = \frac{x'_{Bj} F_2^{N/A}(x_{Bj}/z_1^{(A)}, Q^2)}{x_{Bj} F_2^{N/A}(x'_{Bj}/z_1^{(A)}, Q^2)}. \quad (46)$$

It should be pointed out that, although the r.h.s. of (34) and (46) look formally the same, they differently depend upon the nucleon binding, for, we reiterate, in (34) one has (cf. (18))

$$z_1^{(A)} \simeq 1 - \frac{E_{min}}{M} - \frac{|\vec{P}_{A-1}|^2}{2(A-1)M^2} + \frac{|\vec{P}_{A-1}|}{M} \cos\theta_{\vec{P}_{A-1}\vec{q}}. \quad (47)$$

with  $\vec{P}_{A-1} \equiv -\vec{p}_1$ , whereas in (46), one has (cf. (47))

$$z_1^{(A)} \simeq 1 - \frac{E}{M} - \frac{|\vec{P}_{A-1}|^2}{2(A-1)M^2} - \frac{|\vec{P}_{A-1}|}{M} \cos\theta_{\vec{p}_1\vec{q}}, \quad (48)$$

with  $\vec{P}_{A-1} = -(\vec{p}_2 + \vec{P}_{A-2})$  and  $E$  given by (44). We have seen in Section 3.2 that, due to the small values of  $|\vec{P}_{A-1}|$  and  $E_{min}$ , the process  $A(e, e'(A-1))X$  on a complex nucleus is characterized by  $z_1^{(A)} \simeq 1$ , when  $\theta_{\vec{P}_{A-1}\vec{q}} = 90^\circ$ , with the result that the off-mass-shell dependence of  $F_2^{N/A}$  disappears (cf. the full line for  $^{40}\text{Ca}$  in Fig. 5); the off-mass-shell dependence of  $F_2^{N/A}$  can be enhanced if  $\theta_{\vec{P}_{A-1}\vec{q}} = 180^\circ$ , for an appreciable contribution from the last term of (48) is generated; if so, however, the ratio (34) for a complex nucleus will not appreciably differ from that of the deuteron (cf. the full curves in in Fig. 6), since off-mass-shell effects are solely due to the nucleon momentum  $|\vec{P}_{A-1}|$ , with no contribution from nucleon binding ( $E_{min}/M \ll 1$ ); a totally different situation is expected to occur in the process  $A(e, e'N_2(A-2))X$ ; as a matter of fact, in this case the ‘‘binding term’’  $E/M$

in (48) will generate an appreciable contribution to  $z_1^{(A)}$ , due to the large value of  $|\vec{p}_2|$  associated to nucleon-nucleon correlations (or, equivalently, to high values of the removal energy  $E$ ). Thus, in order to check whether the structure for a deeply bound nucleon would dynamically differ from the one for a weakly bound one, the ratios (34) and (46) for a given nucleus should be plotted versus the same value of  $z_1^{(A)}$ ; in such a way, the off-mass-shell dependence of  $F_2^{N/A}$  is quantitatively the same, but it originates from different contributions to  $z_1^{(A)}$ , viz. the momentum  $\vec{P}_{A-1}$ , for the weakly bound nucleon, and the binding effect  $E$ , for a deeply bound nucleon. If a different behaviour of the two ratios is found, this would represent strong evidence that the structure functions for weakly and deeply bound nucleons are different. Here, again, the  $N_2 - (A-2)$  FSI should be taken into account, although its effect is expected to be canceled in the ratio (46).

Another possibility to investigate the nucleon structure functions would be to analyze the following ratio

$$R_2 = \frac{\sigma_2^A}{\sigma_2^D} = \quad (49) \\ \frac{z_1^{(A)} F_2^{N/A}(x_A, Q^2, p_1^2) n_{cm}^A(|\vec{P}_{A-2}|) n_{rel}^A(|\vec{p}_2 + \vec{P}_{A-2}|)}{z_1^{(D)} F_2^{N/D}(x_D, Q^2, p_1^2) n^D(|\vec{P}_{A-1}| = |\vec{p}_2 + \vec{P}_{A-2}|)}.$$

The results for  $A = 12$  are presented in Fig. 8, in correspondence of two values of  $|\vec{p}_2|$ , for fixed values of the following kinematical variables:  $|\vec{P}_{A-2}| = 50\text{MeV}/c$ ,  $\theta_{\vec{p}_2\vec{q}} = 90^\circ$ ,  $\theta_{\vec{p}_2\vec{P}_{A-2}} = 180^\circ$ , and  $Q^2 = 20\text{GeV}^2/c^2$ ; the full and dashed curves refer to the  $x$ - and  $Q^2$ -rescaling models, respectively. Let us first analyze the results predicted by the first model, viz.  $F_2^{N/A}(x_A, Q^2, p_1^2) \rightarrow F_2^{N/A}(x_{Bj}/z_1^{(A)}, Q^2, p_1^2)$  with  $z_1^{(A)}$  given by (43). The value of the three-momentum of the  $(A-1)$  fragment (a nucleon) in the  $A(e, e'(A-1))X$  cross section off the deuteron, has been chosen the same as the three-momentum of the interacting nucleon  $\vec{P}_{A-1}$  in the case of the  $A(e, e', N_2(A-2))X$  process off  $^{12}\text{C}$ ; by this choice, the removal energy which appears in  $z_1^{(A)}$  (48) is almost equal to the recoil energy appearing in  $z_D$ , so that  $z_1^{(A)} \simeq z_1^D$ ; by this way one should expect a constant behaviour of  $R_2$  (note that  $K_A \simeq K_D$ , for in both cases one has to do with the same values of  $\vec{P}_{A-1}$ ); the deviation from a constant exhibited by the full lines in Fig. 8 is due to the fact that, with the chosen kinematics,  $z_1^{(D)} > z_1^{(A)}$ . Again, the observation of a behaviour different from the one presented in Fig. 8 would indicate a dependence of  $F_2^{N/A}$  upon the binding energy. Let us now consider the prediction by the  $Q^2$ -rescaling model. For the latter, we have considered the model of [19], where the renormalization scale associated to the momentum of a bound nucleon is given by its invariant mass,  $p_1^2 \neq M^2$ . Such an assumption leads to the ansatz  $F_2^{N/A}(x_A, Q^2, p_1^2) = F_2^N(x_A, \xi_A(Q^2, p_1^2)Q^2)$  with  $\xi_A(Q^2, p_1^2) = (M^2/p_1^2)^{(\alpha(p_1^2))/(\alpha(Q^2))}$ , i. e. to an explicit dependence upon the off-shellness of the nucleon. Since the invariant mass of a deeply bound nucleon strongly

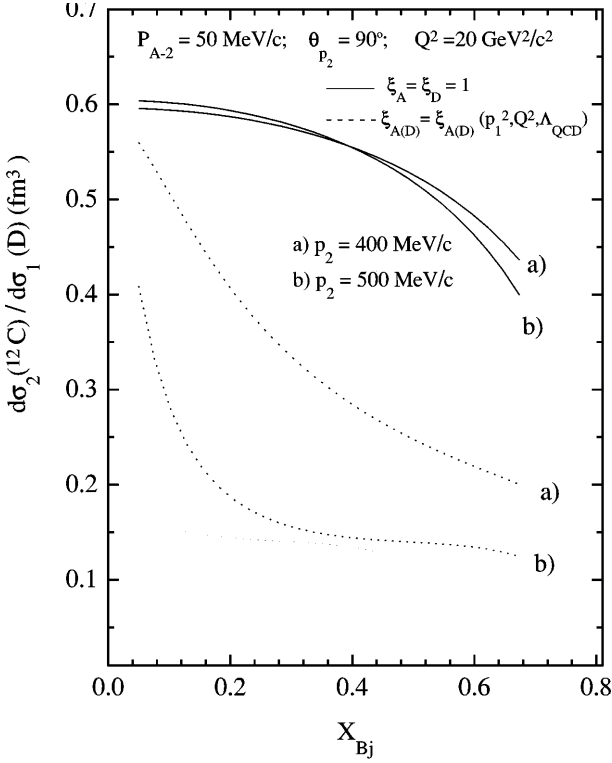


**Fig. 8.** The ratio  $R_2$  (49), for  $^{12}\text{C}$  versus  $x_{Bj}$  for fixed values of: *i*) the momentum of the recoiling  $(A-2)$  system  $P_{A-2} \equiv |\vec{P}_{A-2}| = 50 \text{ MeV}/c$ ; *ii*) the momentum of the recoiling nucleon  $N_2$ ,  $p_2 \equiv |\vec{p}_2| = 400 \text{ MeV}/c$  (a) and  $500 \text{ MeV}/c$  (b); *iii*) the emission angle of nucleon  $N_2$  ( $\theta_{p_2} \equiv \theta_{\vec{p}_2 \vec{q}} = 90^\circ$ ). The full lines correspond to the binding ( $x$ -rescaling) model and the dotted lines to the  $Q^2$ -rescaling model with explicit off-shell dependence of the nucleon structure function

differs from  $M^2$ , the ratio (49) gets the strong  $x_{Bj}$  and  $|\vec{p}_2|$  dependence shown in Fig. 8.

## 5 The local EMC effect

In the binding model ( $x$ -rescaling) of the EMC effect, the slope of the ratio  $R(x_{Bj}, Q^2) = F_2^A(x_{Bj}, Q^2)/(AF_2^N(x_{Bj}, Q^2))$  is generated by the average value of the nucleon removal energy  $\langle E \rangle$ : the larger the value of  $\langle E \rangle$ , the stronger the EMC effect [2]. Since  $NN$  correlations produce high values of  $E$ , and therefore strongly affect the value of  $R$  [21], it would be extremely interesting to measure the so-called *local EMC* (LEMC) effect, i.e., the separate contribution to the ratio  $R$  of the weakly and deeply bound nucleons. Several calculations of the local EMC effect appeared [22,23], and attempts have also been made to compare them with experimental data on neutrino-nucleus DIS [24], but the comparison was not conclusive due to the apparently very large contaminations of the data from non nuclear effects, like e.g. quark fragmentation.

The semi-inclusive  $A(e, e'(A-1))X$  and  $A(e, e', N_2(A-2))X$  processes, offer the possibility to investi-

gate the LEMC effect. As a matter of fact, let us consider the cross sections (9) and (36) for a nucleus  $A$  and the cross section (9) for the deuteron, integrated over a certain interval of  $\vec{P}_{A-1}$ , with  $\vec{P}_{A-1} = -\vec{p}_1$  in (9), and  $\vec{P}_{A-1} = -(\vec{p}_2 + \vec{P}_{A-1})$ , in (36). The following two quantities

$$R_0(x_{Bj}, Q^2) = \frac{\int_a^b \sigma_1^A(x_{Bj}, Q^2, \vec{P}_{A-1}) d\vec{P}_{A-1}}{\int_a^b \sigma_1^D(x_{Bj}, Q^2, \vec{P}_{A-1}) d\vec{P}_{A-1}} \quad (50)$$

$$R_1(x_{Bj}, Q^2) = \frac{\int_a^b \sigma_2^A(x_{Bj}, Q^2, \vec{P}_{A-2}, \vec{p}_2) d\vec{P}_{A-2} d\vec{p}_2}{\int_a^b \sigma_1^D(x_{Bj}, Q^2, \vec{P}_{A-1}) d\vec{P}_{A-1}} \quad (51)$$

will therefore provide the LEMC effect, for they represent the contribution from weakly bound (50) and strongly bound (51) nucleons, respectively [23]. Since the calculation of (51) is a bit involved, we will consider a more restricted type of LEMC, namely the separate contributions of the EMC effect from the various shells of a complex nucleus, i.e. the separate contribution of the various shells to the ratio  $R_0$  [22]. This means that we will assume that the energy resolution in the process  $A(e, e'(A-1))X$  is such, that the contribution to the ratio  $R_0$  due to the ground state, and to the excited states corresponding to the hole state of the target, can experimentally be separated. In what follows the  $^{12}\text{C}$  nucleus will be considered assuming that DIS occurred on a neutron; this means that the final nucleus to be detected is  $^{11}\text{C}$  in the ground state (deep inelastic scattering on a  $p$ -shell neutron) and in an excited state with excitation energy of about  $20 \text{ MeV}$  (deep inelastic scattering on a  $s$ -shell neutron). We have therefore calculated the ratio (50) using realistic Hartree-Fock momentum distributions for the  $s$  and  $p$  shells with single-particle energies  $\epsilon_{0s} = 36 \text{ MeV}$  and  $\epsilon_{0p} = 16 \text{ MeV}$ . The results are presented in Fig. 9, where the usual inclusive EMC ratio, i.e. (50) integrated over the full space, is compared with the separate contribution from the  $s$  and  $p$  shells; it can be seen that, in agreement with [23], the  $s$  shell exhibits a stronger EMC effect, but since in  $^{12}\text{C}$  there are 4  $s$  shell and 8  $p$ -shell nucleons, the total EMC effect is less. In what follows, we will consider the ratio  $R_0$  integrated in a restricted space, viz  $0 < |\vec{P}_{A-1}| < 2 \text{ fm}^{-1}$  and  $0^\circ < \theta_{\vec{P}_{A-1} \vec{q}} < 20^\circ$  (the nucleus  $(A-1)$  is emitted forward) and  $160^\circ < \theta_{\vec{P}_{A-1} \vec{q}} < 180^\circ$  (the nucleus  $(A-1)$  is emitted backward); in Fig. 10 the forward and backward ratios are compared with the full inclusive ratio, and it can be seen that the latter results from the sum of two almost equal contributions. In what follows, only backward emission will be considered, for this is expected to be less affected by FSI between the  $(A-1)$  nucleus and the hadrons resulting from quark hadronisation. The semi-inclusive backward ratio is shown in Fig. 11 together with the separate contributions from the  $s$  and  $p$  shells; it can be seen that not only the shell contributions are well separated, but that the LEMC effect is much larger than the usual EMC effect. In order to give a flavor of the order of magnitude of the cross sections involved, these are presented in Fig. 12.

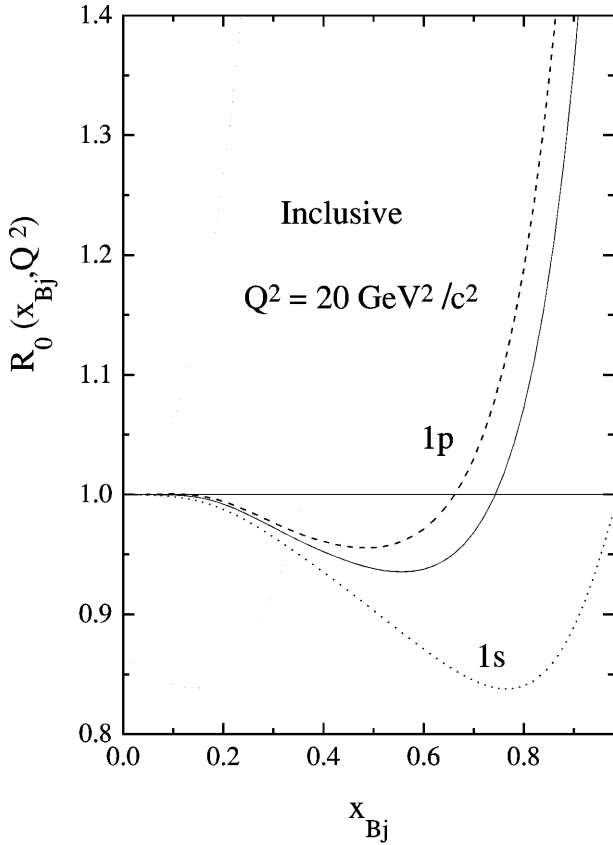


**Fig. 9.** The inclusive local EMC effect in  $^{12}\text{C}$ . The full curve represents the inclusive EMC ratio due to the mean field nucleons in  $^{12}\text{C}$ , i.e. (50) integrated over all space ( $0 \leq P_{A-1} \leq \infty$ ,  $0 \leq \theta_{p_{A-1}} \leq \pi$ ), whereas the dashed and dotted lines represent the contribution from  $1p$  and  $1s$ -shell nucleons, respectively

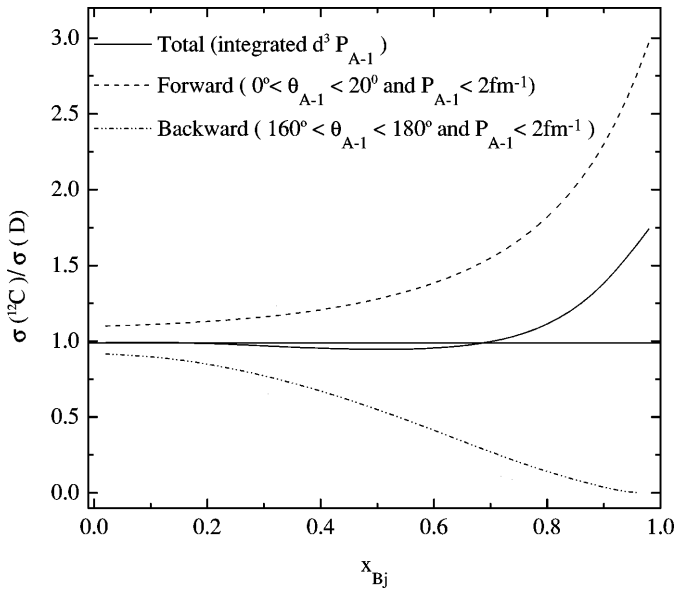


**Fig. 10.** The seminclusive EMC ratio  $\sigma(^{12}\text{C})/\sigma(D) \equiv R_o(x_{Bj}, Q^2)$ , (50) corresponding to nuclei emitted backward and forward, in the kinematical ranges shown in the Figure. The full curve is the usual inclusive EMC ratio

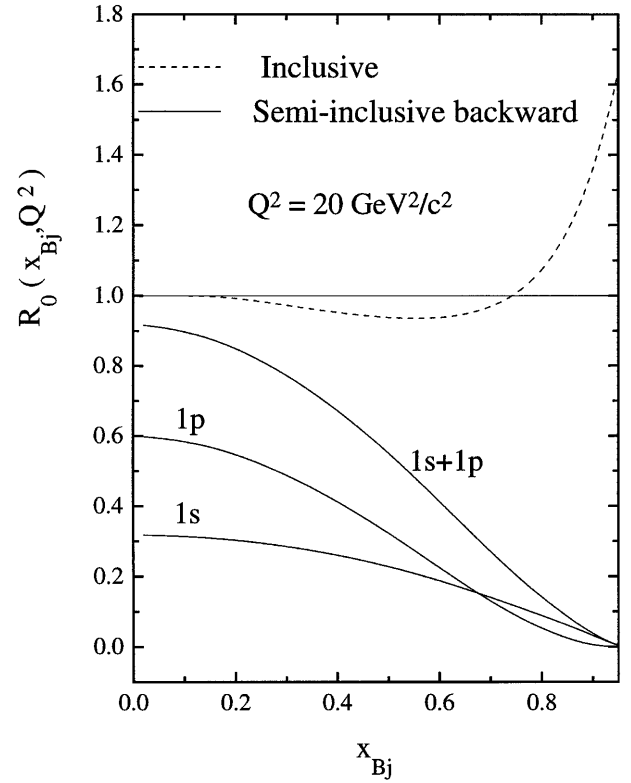


**Fig. 11.** The backward seminclusive local EMC effect on  $^{12}\text{C}$  i.e. the contribution to the ratio  $R_o$  (50) of the nuclei  $(A-1)$  emitted backward in the range  $160^\circ \leq \theta_{A-1} \leq 180^\circ$ ,  $P_{A-1} \leq 2\text{fm}^{-1}$ . The dashed curve represents the usual inclusive EMC ratio ((50), integrated over all space)

## 6 Summary and Conclusions

In the present paper, two new types of semi-inclusive DIS processes of leptons off complex nuclei, have been investigated. The first one, the process  $A(e, e'(A-1))X$ , represents DIS on a shell model, low momentum and low removal energy nucleon, followed by the coherent, low momentum recoil, of the spectator nucleus  $(A-1)$  in the ground, or in a low energy excited state; the second one, the process  $A(e, e'N_2(A-2))X$ , represents DIS on a nucleon  $N_1$  of a correlated pair, followed by the emission of the high momentum nucleon  $N_2$  of the pair, and the low momentum spectator nucleus  $(A-2)$  in the ground, or in a low energy excited state. The experimental investigation of these processes would imply the coincidence detection of  $e'$  and  $(A-1)$ , in the first case, and  $e'$ ,  $N_2$  and  $(A-2)$ , in the second case, respectively. We have demonstrated that both processes can provide relevant information on the following topics:

- i)* the relevance and nature of the FSI between the hadronic jet with the nuclear medium;
- ii)* the validity of the spectator model;
- iii)* the off-shell deformation of the nucleon structure function in the nuclear medium and the  $A$ -dependence of the ratio of the  $n/p$  structure functions;
- iv)* the origin of the EMC effect.

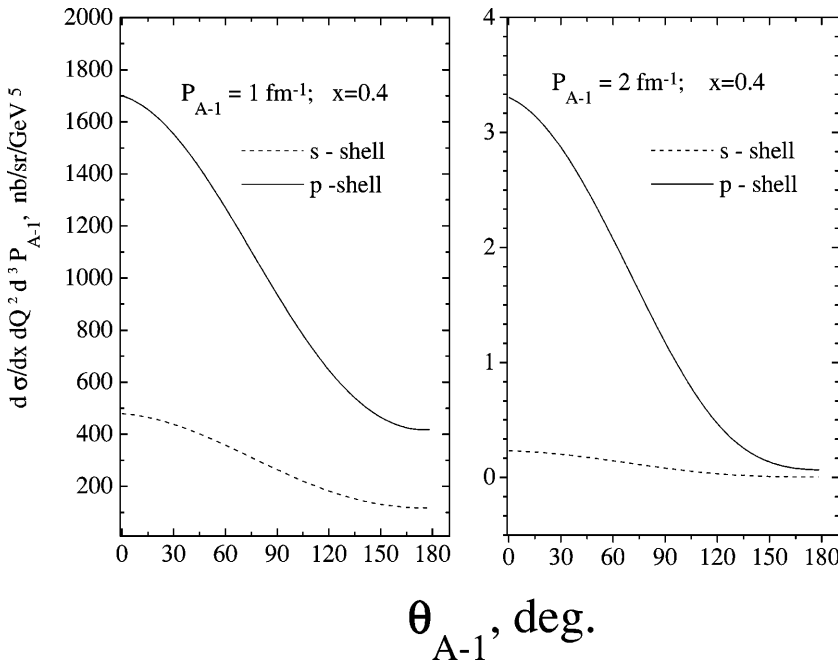


**Fig. 12.** The semi-inclusive cross section (10) resulting from DIS on  $s$ -shell (dashed) and  $p$ -shell (full) nucleons of  $^{12}\text{C}$ . The results are plotted versus the emission angle  $\theta_{P_{A-1}} \equiv \theta_{\widehat{\vec{P}_{A-1}\vec{q}}}$  of the recoiling  $(A-1)$  nuclei, for fixed value of  $x_{Bj} \equiv x$  and in correspondence of two values of the momentum  $P_{A-1} \equiv |\vec{P}_{A-1}|$  of the recoiling  $(A-1)$  nucleus

As a matter of facts :

*i)* if nuclei  $(A-1)$  and  $(A-2)$  are detected in coincidence with the scattered electron, this is a clear signal of the absence of FSI; at the same time, the amount of observed nuclei, i.e. the cross section, will of course depend upon the FSI, therefore the investigation of its absolute value and its dependence upon  $A$ , would allow one to investigate the nature of the FSI, e.g. the hadronisation length of the hit quark;

*ii)* by a proper choice of the kinematics, the ratio of the cross section  $\sigma[A(e, e'(A-1))X]$  to the cross section  $\sigma[D(e, e'N)X]$ , measured versus  $|\vec{P}_{A-1}| = |\vec{p}_N| \equiv |\vec{p}|$ , at a fixed value of the Bjorken scaling variable  $x_{Bj}$ , has been shown to depend, within the Spectator model approach, only upon the low momentum part of the nucleon momentum distributions  $n_A(|\vec{p}|)$  and  $n_D(|\vec{p}|)$ , and since these sharply differ for  $|\vec{p}| \leq 1 \text{ fm}^{-1}$ , the ratio should exhibit a strong  $|\vec{p}|$  dependence (cf. Fig. 2), whose experimental observation would represent a stringent check of the validity of the spectator model. At the same time, the ratio of the cross section  $\sigma[A(e, e'N_2(A-2))X]$  to the cross section  $\sigma[D(e, e'N)X]$  measured versus  $|\vec{p}_{rel}| = |\vec{p}_2 + \vec{P}_{A-2}|/2$  for fixed value of  $|\vec{P}_{A-2}|$  and fixed value of  $x_{Bj}$ , has been shown to depend only upon the relative momentum distributions  $n_{rel}^A(|\vec{p}_{rel}|)$  and  $n^D(|\vec{p}_{rel}|)$ , so that the ratio should exhibit a  $|\vec{p}_{rel}|$  dependence similar for all values of  $A$ , for  $n_{rel}^A \sim n^D$  for  $|\vec{p}_{rel}| \geq 2 \text{ fm}^{-1}$  (cf. Fig. 7); again, the experimental observation of such a scaling behaviour would also represent a stringent test of the Spectator model mechanism;

*iii)* it has been shown that by a proper choice of the kinematics, the ratio of the cross sections for the same nucleus but at two different values of  $x_{Bj}$ , becomes independent of the nuclear quantities, being determined only by the nucleon structure function; it has therefore been

demonstrated, in the case of the process  $A(e, e'(A-1))X$ , that such a ratio could provide significant information on different models of the structure function of weakly bound nucleons (cf. Figs. 5 and 6). Eventually (cf. Fig. 8) it has been shown that the ratio of the cross section for the process  $A(e, e'N_2(A-2))X$  to the deuteron cross section, could provide information on the *binding energy dependence* of the nucleon structure functions;

*iv)* the local EMC effect has been investigated (cf. Figs. 9-12), pointing out that that the processes  $A(e, e'(A-1))X$  and  $A(e, e'N_2(A-2))X$  integrated over a proper value of the momenta of the detected particles  $(A-1, N_2$  and  $A-2)$  will provide, for the first time, the separate contribution to the EMC ratio of the weakly and deeply bound nucleons, thus providing a stringent check of the binding model (x-rescaling) of the EMC effect. Detailed calculations have been performed for the process  $A(e, e'(A-1))X$ , demonstrating that in the binding model, the inclusive EMC effect results from the cancellation of two large contributions from the forward and backward emitted  $(A-1)$  nuclei (cf. Fig. 10); therefore, a significant check of the binding model could be provided by the measurement of the backward ratio which exhibits a 60 percent deviation from unity instead of the 10 percent deviation of the usual inclusive EMC effect (cf. Fig. 11).

In closing, we would like to point out that the results we have exhibited have been obtained with non relativistic momentum distributions and spectral functions. Calculations for the two- and three-body systems including relativistic effects by a full covariant Bethe-Salpeter approach and by light-cone spectral functions, respectively, will be presented elsewhere ([25], [26]).

We gratefully acknowledge Boris Kopeliovitch and Daniele Treleani for useful comments and discussions. L.P.K. thanks INFN

Sezione di Perugia for warm hospitality and financial support. S.S. thanks the TMR programme of the European Commission ERB FMR-CT96-008, INFN Sezione di Perugia and Department of Physics, University of Perugia for partial financial support.

## A The electron-hadron cross section

In this Appendix the derivation of the semi-inclusive electron-hadron cross section within the instant-form dynamics will be presented.

In the one-photon exchange approximation the cross section describing the scattering of an electron  $e$  from a hadron  $A$  reads as follows:

$$d\sigma = \frac{M_A m_e}{(P_A \cdot k_e)} (2\pi)^4 \delta^{(4)}(P_A + k_e - k_{e'} - P_f) \times \left| \langle k_{e'} | \hat{j}^\mu(0) | k_e \rangle \frac{1}{Q^2} \langle P_A | \hat{J}_\mu^A(0) | P_f \rangle \right|^2 \times \frac{m_e d^3 k_{e'}}{\mathcal{E}_{k'} (2\pi)^3} d\tau_f, \quad (\text{A1})$$

where  $\hat{j}^\mu(0)$  and  $\hat{J}_\mu^A(0)$  are the electromagnetic current operators for the lepton and the hadron, respectively,  $M_A$  ( $P_A$ ,  $E_A$ ), and  $m_e$  ( $k_e$ ,  $\mathcal{E}_{k'}$ ) stand for the masses (4-momenta, total energy) of the hadron and the electron in the initial state,  $k_{e'}$  and  $P_f$  denote the four-momenta of the electron and the hadron in the final state,  $Q^2 = -q^2 = -(k_e - k_{e'})^2 = \vec{q}^2 - \nu^2 = 4\mathcal{E}_k \mathcal{E}_{k'} \sin^2 \frac{\theta}{2}$  is the 4-momentum transfer, (with  $\vec{q} = \vec{k}_e - \vec{k}_{e'}$ ,  $\nu = \mathcal{E}_k - \mathcal{E}_{k'}$  and  $\theta \equiv \theta_{\vec{k}_e \vec{k}_{e'}}$ ), and  $d\tau_f$  the phase space volume of all particles (but the scattered electron) in the final state. In (A1) the following normalization conditions are used:

$$\Lambda_+(p) = \frac{\hat{p} + M}{2M}, \quad \langle p | p' \rangle = \frac{E}{M} (2\pi)^3 \delta^3(\vec{p} - \vec{p}'),$$

$$\bar{u} u = 1, \quad u^+ u = \frac{E}{M}. \quad (\text{A2})$$

where  $M$  is the nucleon mass.

### A.1 The inclusive cross-section

By placing in (A1)  $f \equiv X$  and  $d\tau_f = 1$ , in the lab system, the cross section for the inclusive process  $A(e, e')X$ , i. e. when only the scattered electron is detected, is obtained

$$\frac{d\sigma}{d\Omega' d\mathcal{E}_{k'}} = \frac{4\alpha^2 \mathcal{E}_{k'}}{Q^4 \mathcal{E}_k} \frac{1}{2} L^{\mu\nu} W_{\mu\nu}^A \quad (\text{A3})$$

where the leptonic tensor,  $L_{\mu\nu}$ , is

$$L_{\mu\nu} = k_\mu k'_\nu + k'_\mu k_\nu - g_{\mu\nu} (k \cdot k'), \quad (\text{A4})$$

and the hadronic tensor,  $W_{\mu\nu}^A$ , is

$$W_{\mu\nu}^A = \frac{1}{4\pi} \sum_{\alpha_A} \sum_X (2\pi)^4 \delta^{(4)}(P_A + q - p_X) \langle \alpha_A, \vec{P}_A = 0 | J_\mu^A(0) | \alpha_X \vec{p}_X \rangle \langle \alpha_X \vec{p}_X | J_\nu^A(0) | \alpha_A, \vec{P}_A = 0 \rangle. \quad (\text{A5})$$

The general form of the hadronic tensor, restricted by requirements of gauge-invariance, time-reversal invariance and parity conservation, depends upon two structure functions  $W_i^A$ , corresponding to the two independent scalars of the problem, viz.

$$W_{\mu\nu}^A = W_1^A(\nu, Q^2) \left[ g_{\mu\nu} + \frac{q_\mu q_\nu}{Q^2} \right] + \frac{W_2^A(\nu, Q^2)}{M^2} \tilde{P}_\mu^A \tilde{P}_\nu^A \quad (\text{A6})$$

where  $\tilde{P}_\mu^A = p_\mu^A + \frac{q_\mu (p^A \cdot q)}{Q^2}$ .

The contraction of the two tensors gives the well known result:

$$\frac{d\sigma}{d\Omega' d\mathcal{E}_{k'}} = \sigma_{Mott} \left[ W_2^A(\nu, Q^2) + 2W_1^A(\nu, Q^2) \tan^2 \frac{\theta}{2} \right] \quad (\text{A7})$$

where

$$\sigma_{Mott} = \left( \frac{\alpha \cos \frac{\theta}{2}}{2\mathcal{E}_k \sin^2 \frac{\theta}{2}} \right)^2 \quad (\text{A8})$$

is the Mott cross section. Note that the inclusive process on the nucleon  $N(e, e')X$ , is described by the above formulae with  $A = N$ ,  $P^A = p^N$ .

### A.2 The semi-inclusive cross-section

Let us now discuss the semi-inclusive process of the type  $A(e, e')B)X$ , when another hadron  $B$  is detected in coincidence with the electron. We have in this case  $f \equiv (B, X)$  and  $d\tau_f = \frac{M_B d^3 P_B}{E_B (2\pi)^3}$ . The relevant hadronic four-momenta involved in the process are  $P_B \equiv (P_B^0, \vec{P}_B)$ , with  $P_B^0 = \sqrt{(M_B + E_B^*)^2 + \vec{P}_B^2}$ ,  $M_B$  and  $E_B^*$  being, respectively, the rest mass and the intrinsic excitation energy of  $B$ , and  $p_X \equiv (p_X^0, \vec{p}_X)$ , with  $p_X^0 = \sqrt{M_X^2 + \vec{p}_X^2}$ . The cross-section in IA is given by

$$\frac{d^4\sigma}{d\Omega' d\mathcal{E}_{k'} dE_B d\Omega_B} = \frac{4\alpha^2 \mathcal{E}_{k'}}{Q^4 \mathcal{E}_k} \frac{|\vec{P}_B| E_B}{M_B} L^{\mu\nu} W_{\mu\nu}^{A,s.i.} \quad (\text{A9})$$

where the form of the leptonic tensor is again given by (A4), but the hadronic tensor will have a more complex structure, viz:

$$W_{\mu\nu}^{A,s.i.} = \frac{1}{4\pi} \sum_{\alpha_A} \sum_{\alpha_B, X} (2\pi)^4 \delta^{(4)}(P_A + q - P_B - p_X) \langle \alpha_A \vec{P}_A = 0 | J_\mu^A(0) | \alpha_X \vec{p}_X, \alpha_B \vec{P}_B E_B^* \rangle \langle \alpha_B \vec{P}_B E_B^*, \alpha_X \vec{p}_X | J_\nu^A(0) | \alpha_A \vec{P}_A = 0 \rangle, \quad (\text{A10})$$

where the sum over  $X$  stands for a sum over the discrete and an integral over the continuum quantum numbers of  $X$ ,  $\alpha_B$  stands for the discrete and continuum quantum numbers of the final nucleus, and the vector  $|\alpha_X \vec{p}_X, \alpha_B \vec{P}_B E_B^* \rangle$  consists asymptotically of a nucleus

$B$  detected with momentum  $\vec{P}_B$  and intrinsic excitation energy  $E_B^*$ , and an undetected hadronic state  $X$ . For the semi-inclusive process we are considering, the general form of the hadronic tensor, restricted by requirements of gauge-invariance, time-reversal invariance and parity conservation, depends on four structure functions  $W_i^A$ , corresponding to the four independent scalars of the problem, viz. (see e.g. [27] and [30] and references therein quoted)

$$\begin{aligned} W_{\mu\nu}^{A,s.i.} = & -W_1^A g_{\mu\nu} + \frac{W_2^A}{M^2} P_\mu^A P_\nu^A \\ & + W_3^A \frac{1}{(p \cdot P^A)} \frac{1}{2} (P_\mu^A p'_\nu + P_\nu^A p'_\mu) \\ & + \frac{W_4^A}{M^2} p'_\mu p'_\nu \end{aligned} \quad (\text{A11})$$

where the terms linear in  $q^\mu$  do not appear thanks to the gauge invariance of the leptonic tensor. The structure of  $W_{\mu\nu}^{A,s.i.}$  can be obtained in a more physically transparent way, by introducing, instead of  $W_{1-4}$ , another set of four scalar response functions. To this end, the complete set of polarization 4-vectors for a virtual photon

$$\epsilon_\pm^\mu = \mp \frac{1}{\sqrt{2}}(0, 1, \pm i, 0), \quad \epsilon_0^\mu = \frac{1}{\sqrt{Q^2}}(|\vec{q}|, 0, 0, q_0) \quad (\text{A12})$$

is introduced, with  $\epsilon_\mu q^\mu = 0$ ,  $\sum_\lambda \epsilon_\lambda^{*\mu} \epsilon_\lambda^\nu = -g^{\mu\nu} + \frac{q^\mu q^\nu}{q^2}$ , and  $\epsilon_\lambda^* = (-1)^\lambda \epsilon_{-\lambda}$  ( $\lambda = \pm, 0$ ), to obtain

$$L^{\mu\nu} W_{\mu\nu}^{A,s.i.} = \sum_{\lambda\lambda'} L_{\lambda\lambda'} W_{\lambda\lambda'}, \quad (\text{A13})$$

where

$$\begin{aligned} L_{\lambda\lambda'} &= \epsilon_\lambda^{*\mu} L_{\mu\nu} \epsilon_{\lambda'}^{\nu}, \\ W_{\lambda\lambda'} &= (-1)^{\lambda+\lambda'} \epsilon_\lambda^{*\mu} W_{\mu\nu}^{A,s.i.} \epsilon_{\lambda'}^\nu. \end{aligned} \quad (\text{A14})$$

Due to time-reversal and parity invariances of the electromagnetic interaction, only four independent combinations of  $\lambda\lambda'$  will appear in (A13), which are usually chosen in the following form:

$$\begin{aligned} W_L^A &= \frac{|\vec{q}|^2}{Q^2} W_{00}; \\ W_T^A &= W_{11} + W_{-1-1}; \\ W_{LT}^A &= \frac{|\vec{q}|}{\sqrt{Q^2}} 2\text{Re}[W_{01} - W_{0-1}]; \\ W_{TT}^A &= -2\text{Re} W_{1-1}; \end{aligned} \quad (\text{A15})$$

defining, respectively, the longitudinal ( $L$ ), transverse ( $T$ ), longitudinal-transverse ( $LT$ ) interference and transverse-transverse ( $TT$ ) nuclear response functions. The corresponding parts of the leptonic tensor can be straightforwardly found by subtracting a factor  $4\mathcal{E}\mathcal{E}' \cos^2 \theta/2$  from  $L_{\lambda\lambda'}$ , (A14), i.e. by defining a ‘‘reduced’’ leptonic tensor  $L_{\lambda\lambda'} = 4\mathcal{E}\mathcal{E}' \cos^2 \theta/2 l_{\lambda\lambda'}$ . One finds

$$l_{00} = \frac{Q^2}{|\vec{q}|^2};$$

$$\begin{aligned} l_{11} &= \frac{Q^2}{2|\vec{q}|^2} + \tan^2 \frac{\theta}{2}; \\ l_{01} &= \frac{1}{\sqrt{2}} \frac{\sqrt{Q^2}}{|\vec{q}|} \left( \frac{Q^2}{|\vec{q}|^2} + \tan^2 \frac{\theta}{2} \right)^{1/2}; \\ l_{1-1} &= -\frac{Q^2}{2|\vec{q}|^2} \end{aligned} \quad (\text{A16})$$

and the cross section assumes the well-known form (see e.g. [30] who considered the process  $A(e, e'p)X$  in the quasi-elastic region):

$$\begin{aligned} \frac{d^4\sigma}{d\Omega' d\mathcal{E}_k' dE_B d\Omega_B} = & \sigma_{Mott} |\vec{p}_B| E_B \\ & \times \sum_i V_i W_i^A(\nu, Q^2, \vec{p}_B, E_B^f) \end{aligned} \quad (\text{A17})$$

where  $i \equiv \{L, T, LT, TT\}$ , and the kinematical factors  $V_i$ , in agreement with the definitions (A15), (A16), have the following form:

$$\begin{aligned} V_L &= \frac{Q^4}{|\vec{q}|^4}, \\ V_T &= \tan^2(\theta/2) + \frac{Q^2}{2|\vec{q}|^2}, \\ V_{LT} &= \frac{Q^2}{\sqrt{2}|\vec{q}|^2} \sqrt{\tan^2(\theta/2) + \frac{Q^2}{|\vec{q}|^2}}, \\ V_{TT} &= \frac{Q^2}{2|\vec{q}|^2}. \end{aligned} \quad (\text{A18})$$

The nuclear response functions  $W_i^A$  can be expressed in term of nuclear dynamics, once a model for the nuclear current operators  $J_\mu^A(0)$ , appearing in (A8), is assumed. Nowadays, there is no rigorous quantum field theory to describe, from first principles, a many body hadronic system. Usually, in electromagnetic processes, the nuclear responses are related to the nucleon responses by some models, the simplest one being the *impulse approximation* (IA). The IA is based on the following assumptions:

1. The nuclear current operator is the sum of one-body nucleon operators

$$J_\nu^A(Q^2) = \sum_{N=1}^A J_\nu^N(Q^2), \quad (\text{A19})$$

i.e. the sum of currents for Dirac particles treated within an effective quantum field theory, i.e. with their internal structure described by some phenomenological form factors; therefore the effective current operators for nucleons are  $Q^2$ -dependent and so is the nuclear current operator, where the  $Q^2$ -dependence in the r.h.s. and l.h.s. of (A19) can in principle differ;

2. the final hadronic state  $|\alpha_X p_X, \alpha_B \vec{P}_B E_B^*\rangle$  asymptotically consists of two non interacting (i.e. plane wave states) systems, i.e.

$$|\alpha_X p_X, \alpha_B \vec{P}_B E_B^*\rangle = \hat{A} \{ |\alpha_X p_X\rangle |\alpha_B \vec{P}_B E_B^*\rangle \}, \quad (\text{A20})$$

where  $\hat{A}$  is a proper antisymmetrization operator;

3. the incoherent contributions leading to the emission of  $X$ , due to the interaction of  $\gamma^*$  with  $B$ , are disregarded.

It is straightforward to show that if one adheres to the above assumptions, inserts in (A10) a complete set of plane wave nucleon states, and assumes the conservation of linear momentum by using translationally invariant nuclear wave functions, i.e.

$$\begin{aligned} \langle \alpha_A \vec{P}_A | \{ | \alpha_N \vec{p}_N \rangle | \alpha_B \vec{P}_B E_B^* \rangle \} = \\ \delta(\vec{P}_A - \vec{p}_N - \vec{P}_B) \delta_{\alpha_A, \alpha_N + \alpha_B} \\ \langle \alpha_A \vec{P}_A | \alpha_N \vec{p}_N, \alpha_B \vec{P}_A - \vec{p}_N E_B^* \rangle, \end{aligned} \quad (\text{A21})$$

then in the lab system, the contribution from protons ( $t_N = 1/2$ ) or neutrons ( $t_N = -1/2$ ) to the hadronic tensor becomes ( $\vec{p}_N = -\vec{P}_B$ ):

$$\begin{aligned} W_{\mu\nu}^{A,s.i.,t_N}(\nu, Q^2, \vec{p}_N) = \frac{1}{4\pi} \frac{M}{E_{\vec{p}_N}} \frac{1}{2} \sum_{s_N} \sum_{\alpha_X} \\ \int d\vec{p}_X \langle \alpha_N \vec{p}_N | J_\mu^N(0) | \alpha_X p_X \rangle \langle \alpha_X p_X | J_\nu^N(0) | \alpha_N \vec{p}_N \rangle \\ \delta(M_A + \nu - p_n^0 - p_X^0) \delta(\vec{q} + \vec{p}_N - \vec{p}_X) n_{E_B^*}^{t_N}(|\vec{p}_N|) \end{aligned} \quad (\text{A22})$$

where

$$\begin{aligned} n_{E_B^*}^{t_N}(|\vec{p}_N|) = A \sum_{\alpha_A} \sum_{\alpha_B} \left| \langle \alpha_A \vec{P}_A = 0 | \alpha_N \vec{p}_N; \alpha_B - \vec{p}_N E_B^* \rangle \right|^2 \\ \delta_{\alpha_A, \alpha_N + \alpha_B} \end{aligned} \quad (\text{A23})$$

represents the nucleon momentum distribution (assumed to be independent of  $s_N$ ), corresponding to the intrinsic excitation energy  $E_B^*$  of  $B$ . Introducing the nucleon spectral function

$$\begin{aligned} P_N^{t_N}(|\vec{p}_N|, E) = \\ A \sum_{\alpha_A} \sum_{\alpha_B} \sum_f \left| \langle \alpha_A \vec{P}_A = 0 | \alpha_N \vec{p}_N; \alpha_B - \vec{p}_N E_B^f \rangle \right|^2 \\ \delta(E - (E_B^f - E_A^0)) \delta_{\alpha_A, \alpha_N + \alpha_B}, \end{aligned} \quad (\text{A24})$$

we can write

$$n_{E_B^*}^{t_N}(|\vec{p}_N|) = \int dE P_N^{t_N}(|\vec{p}_N|, E) \delta_{E_B^f, E_B^0 + E_B^*} \quad (\text{A25})$$

where we have considered only the discrete excited states of  $B$ . Due to our ignorance of the nucleon current matrix elements in the nuclear tensor (A22), a common practice is to express the latter in term of the nucleon tensor ((A5),  $A = N$ ); however, whereas the three-momentum conservation is the same in (A5) and (A22), the energy conservation is not, being, respectively,  $\nu + M_A = \sqrt{(M_B + E_B^*)^2 + \vec{p}_N^2} - \sqrt{\vec{p}_X^2 + M_X^2}$  in (A22), and  $\nu + E_{\vec{p}_N} = E_{\vec{p}_N + \vec{q}}$  in (A5); as a result, the nuclear tensor cannot be directly related to the nucleon one, unless some additional, *ad hoc* assumptions are made. To this end, two main prescriptions have been proposed :

1. the hit nucleon is considered to be on-shell, i.e. with a four momentum equal to the one of a free nucleon  $p_N^{on} = (\sqrt{\vec{p}_N^2 + M^2}, \vec{p}_N)$  and in (A22) the replacement  $\nu \longrightarrow \bar{\nu} = \nu + M_A - \sqrt{(M_B + E_B^*)^2 + \vec{p}_N^2} - \sqrt{\vec{p}_N^2 + M^2}$  is done, so that  $\delta(M_A + \nu - P_B^0 - p_X^0) \longrightarrow \delta(\sqrt{\vec{p}_N^2 + M^2} + \bar{\nu} - p_X^0)$ ; by this way, the electromagnetic vertex of the nuclear tensor (A22) corresponds to that of a free nucleon, evaluated at the same  $\vec{q}$ , but at the transferred energy  $\bar{\nu}$  instead of  $\nu$  [28–30], which means that the nucleon hadronic tensor (A5) has to be evaluated for  $p_N = p_N^{on}$  and  $Q_N^2 = \bar{Q}^2 = \vec{q}^2 - \bar{\nu}^2 \neq Q^2$ .
2. The hit nucleon is considered off-shell, with four-momentum  $p_N^{off} = (p_N^0, \vec{p}_N)$  with  $p_N^0 = M_A - \sqrt{(M_B + E_B^*)^2 + \vec{p}_N^2}$  and  $\delta(M_A + \nu - P_B^0 - p_X^0) \longrightarrow \delta(p_N^0 + \nu - p_X^0)$ , which means that the nucleon hadronic tensor (A5) has to be evaluated for  $p_N = p_N^{off}$  and  $Q_N^2 = \vec{q}^2 - \nu^2 = Q^2$ .

In both cases the nuclear tensor (A22) can be expressed through the nucleonic tensor (A5) obtaining:

$$\begin{aligned} W_{\mu\nu}^{A,s.i.,t_N}(\nu, Q^2, \vec{p}_N) = W_{\mu\nu}^N(p_N \cdot q, Q_N^2, p_N^2) \\ \times \frac{M}{E_{\vec{p}_N}} n_{E_B^*}^{t_N}(|\vec{p}_N|) \end{aligned} \quad (\text{A26})$$

As discussed in details in [29], both choices imply the presence of many-body currents, due to the dependence of  $p_n^{off}$  and  $\bar{\nu}$  upon the four-momentum of the nucleus. Then, it has also been stressed that the instant-form dynamics (used in the present paper) does not mandate one or the other choice. A comparison of both procedures will be presented elsewhere ([25]); in the present paper choice 2 has been adopted, and the  $Q^2$  dependence of the hadronic tensor for an off mass shell nucleon is assumed to be the same as for the free one, i.e.

$$\begin{aligned} W_{\mu\nu}^{t_N}(p_N \cdot q, Q_N^2) = -W_1^N(p_N \cdot q, Q_N^2) \left[ g_{\mu\nu} + \frac{q_\mu q_\nu}{Q^2} \right] \\ + \frac{W_2^N(p_N \cdot q, Q_N^2)}{M^2} \tilde{p}_\mu \tilde{p}_\nu. \end{aligned} \quad (\text{A27})$$

Inserting (A27) into (A26) and the latter into (A14), one gets for the nuclear response functions (A15):

$$\begin{aligned} W_i^A(\nu, Q^2, \vec{p}_N) = \frac{M}{E_{\vec{p}_N}} n_{E_B^*}(|\vec{p}_N|) \\ \cdot \sum_{\alpha=1,2} C_i^\alpha(\nu, Q^2, p_N) \\ \cdot W_\alpha^N(p_N \cdot q, Q_N^2) \end{aligned} \quad (\text{A28})$$

with the coefficients  $C_i^\alpha(\nu, Q^2, p_N)$  straightforwardly obtained from (A15) and (A18), viz.



$$\begin{aligned}
C_L^1 &= -\frac{|\vec{q}|^2}{Q^2} \\
C_L^2 &= \frac{|\vec{q}|^4}{Q^4} \left[ \frac{p_N^0 |\vec{q}| + \nu |\vec{P}_B| \cos(\theta_{\vec{P}_B \vec{q}})}{M |\vec{q}|} \right]^2 \\
C_T^1 &= 2 \\
C_T^2 &= \left( \frac{|\vec{P}_B| \sin(\theta_{\vec{P}_B \vec{q}})}{M} \right)^2 \\
C_{LT}^1 &= 0 \\
C_{LT}^2 &= \frac{|\vec{q}|^2 \sqrt{8} |\vec{p}_N| \sin(\theta_{\vec{P}_B \vec{q}})}{Q^2 M} \\
&\quad \cdot \frac{p_N^0 |\vec{q}| + \nu |\vec{P}_B| \cos(\theta_{\vec{P}_B \vec{q}})}{M |\vec{q}|} \cos(\phi_B) \\
C_{TT}^1 &= 0 \\
C_{TT}^2 &= \frac{1}{2} \left( \frac{|\vec{P}_B| \sin(\theta_{\vec{P}_B \vec{q}})}{M} \right)^2 \cos(2\phi_B) \quad (\text{A29})
\end{aligned}$$

where  $\phi_B$  is the azimuthal angle of  $\vec{P}_B$ . Changing variables from  $\nu$ ,  $Q^2$ , and  $(p_N \cdot q)$  to  $x_{Bj} = Q^2/(2M\nu)$ ,  $Q^2$ , and  $x_A = Q^2/2(p_N \cdot q)$ , introducing the usual structure functions  $F_1 = MW_1$  and  $F_2 = \frac{p_N \cdot q}{M} W_2$ , using the Callan–Gross relation,  $F_2 = 2xF_1$ , and placing (A28) into (A17), (9) is obtained, where  $p_N \equiv p_1$  and  $B = (A - 1)$ .

The hadronic tensor for the second process we are considering, viz.  $A(e, e' B_1 B_2) X$ , with  $B_1 = N_1$  and  $B_2 = (A - 2)$ , will depend upon six response functions which are given by proper bilinear combinations of the Fourier transforms of the transition matrix elements of the nuclear current operator (see e.g. [27]). By following the procedure described above and by introducing the two-nucleon spectral function (7), (36) can be readily obtained.

## References

1. M. Arneodo, Phys. Rep., **240** (1994) 393
2. L.L. Frankfurt and M.I. Strikman, Phys. Rep. 160 (1988) 235
3. A.G. Tenner and N.N. Nikolaev, Nuovo Cim. A105 (1992) 1001
4. G.D. Bosveld, A.E.L. Dieperink and O. Schölten, Phys. Rev. C 45 (1992) 2616
5. C. Ciofi degli Atti and S. Simula, Phys. Lett. B 319 (1994) 23; Few Body Syst. 18 (1995) 555
6. S.E. Khun and K.A. Griffioen (spokespersons), CEBAF proposal PR-94-102
7. S. Simula, Phys. Lett. B 387 (1996) 245; W. Melnitchouk, M. Sargsian, M.I. Strikman, Z. Phys. A359 (1997) 99
8. C. Ciofi degli Atti, L.P. Kaptari and S. Scopetta, e-print archives **nucl-th/9609062**
9. Proceedings of the workshop “Physics at HERA”, Sept. 1995 - May 1996, DESY, Hamburg, 1996
10. V. Metag, D. v. Harrach and A. Schäfer; the workshop “Long Term Perspectives of GSI” 1996, (unpublished), private communication
11. C. Ciofi degli Atti and S. Liuti, Phys. Lett. B225 (1989) 215
12. C. Ciofi degli Atti, S. Simula, L.L. Frankfurt and M.I. Strikman, Phys. Rev. C 44 (1991) R7
13. C. Ciofi degli Atti and S. Simula, Phys. Rev. C 53 (1996) 1689
14. M. Baldo, M. Borromeo and C. Ciofi degli Atti, Nucl. Phys. A 604 (1996) 429
15. F.E. Close, R.G. Roberts and G.G. Ross, Nucl. Phys. B 296 (1988) 582
16. M.I. Strikman, M. Tverskoy and M. Zhalov, in preparation
17. M.R. Adams *et al.*, Phys. Rev. Lett. 74 (1995) 5198
18. A.Yu. Umnikov, L.P. Kaptari and F. Khanna, Phys. Rev. C 53 (1996) 377
19. G.V. Dunne and A.W. Thomas, Nucl. Phys. A 455 (1986) 701-719; W. Melnitchouk, A.W. Schreiber and A.W. Thomas, Phys. Rev. D 49 (1994) 1199; S.A. Kulagin, G. Piller and W. Weise, Phys. Rev. D 50 (1994) 1154
20. J.G. Zabolitzky and W. Ey, Phys. Lett. B 76 (1978) 527; R. Schiavilla, V.R. Pandharipande and R.B. Wiringa, Nucl. Phys. A 449 (1986) 219
21. C. Ciofi degli Atti and S. Liuti, Phys. Rev. C 41 (1990) 1100
22. S. Kumano and F.E. Close, Phys. Rev. C 41 (1990) 1855
23. C. Ciofi degli Atti and S. Liuti, Nucl. Phys. A 532 (1991) C241
24. T. Kitagaki *et al.* Phys. Lett. B214 (1988) 281
25. C. Ciofi degli Atti, S. Scopetta, L. Kaptari and A. Umnikov, in preparation
26. C. Ciofi degli Atti, A. Umnikov and M. Strikman, to appear
27. S. Boffi, C. Giusti and F.D. Pacati, Phys. Rept. 226 (1993) 1
28. L. Heller and A. W. Thomas, Phys. Rev. C 41 (1990) 2756
29. U. Oelfke, P.U. Sauer and F. Coester, Nucl. Phys. A518 (1990) 593
30. T. De Forest, Jr. Nucl. Phys. A392 (1983) 232